

## Supporting Information

For

### Enhancing Electrocatalytic Water Oxidation: Ligand Complementarity in Ternary Cu(II) Complexes

Pranjal Das,<sup>a,b</sup> Hemrupa Kuilya,<sup>a</sup> Swati Basak,<sup>a,b</sup> Baisali Hazarika<sup>a,b</sup>, Joydeep Ray,<sup>c</sup> Debajit  
Sarma,<sup>c</sup> Diganta Choudhury,<sup>a</sup> and Apurba Kalita <sup>\*,a</sup>

<sup>a</sup>*Department of Chemistry, B. Borooah College, Guwahati, Assam 781007, India*

<sup>b</sup>*Department of Chemistry, Gauhati University, Guwahati 781014, Assam, India*

<sup>c</sup>*Department of Chemistry, Indian Institute of Technology Patna, Patna 801103, Bihar, India*

## Table of Contents:

Sl. No.	Contents	Page No.
1	Experimental Procedures	8
2	Electron count in redox peak using Laviron equations	9
3	Calculation of Faradic efficiency	9
4	Synthesis of $[\text{Cu}(\text{bipy})_2](\text{ClO}_4)_2$	10
5	Synthesis of $[\text{Cu}(\text{Phen})_2](\text{ClO}_4)_2$	10
6	Synthesis of $[\text{Zn}(\text{bipy})(\text{HL}_1)](\text{ClO}_4)_2$	10
7	Synthesis of $[\text{Zn}(\text{phen})(\text{HL}_1)](\text{ClO}_4)_2$	11
8	Controlled potential electrolysis of complexes 4 and 5	11
9	<b>Fig. S1</b> ORTEP diagram (50% thermal ellipsoid plot) of (a) complex 3 and (b) complex 4. Counterions, hydrogen atoms and solvent molecules are removed for clarity.	12
10	<b>Fig. S2</b> ORTEP diagram (50% thermal ellipsoid plot) of (a) complex 5 and (b) complex 6. Counterions, hydrogen atoms and solvent molecules are removed for clarity.	12
11	<b>Fig. S3</b> ORTEP diagram (50% thermal ellipsoid plot) of (a) complex $[\text{Zn}(\text{bipy})(\text{HL}_1)](\text{ClO}_4)_2$ and (b) complex $[\text{Zn}(\text{phen})(\text{HL}_1)](\text{ClO}_4)_2$ . Counterions, hydrogen atoms and solvent molecules are removed for clarity.	13
12	<b>Fig. S4</b> FT-IR spectra of (a) complex 1 and (b) complex 2 in KBr.	13
13	<b>Fig. S5</b> FT-IR spectra of (a) complex 3 and (b) complex 4 in KBr.	14
14	<b>Fig. S6</b> FT-IR spectra of (a) complex 5 and (b) complex 6 in KBr.	14
15	<b>Fig. S7</b> FT-IR spectra of (a) complex 7 and (b) complex $[\text{Zn}(\text{bipy})(\text{HL}_1)](\text{ClO}_4)_2$ in KBr.	15
16	<b>Fig. S8</b> FT-IR spectra of (a) complex $[\text{Zn}(\text{phen})(\text{HL}_1)](\text{ClO}_4)_2$ and (b) complex $[\text{Cu}(\text{bipy})_2](\text{ClO}_4)_2$ in KBr.	15
17	<b>Fig. S9</b> FT-IR spectrum of complex $[\text{Cu}(\text{phen})_2](\text{ClO}_4)_2$ in KBr.	16
18	<b>Fig. S10</b> PXRD patterns of (a) complex 1 and (b) complex 2.	16
19	<b>Fig. S11</b> PXRD patterns of (a) complex 4 and (b) complex 5.	17
20	<b>Fig. S12</b> PXRD patterns of complex 6.	17
21	<b>Fig. S13</b> (a) UV-visible spectra of 1 mM solution of complex 1 (red line) and complex 2 (blue line) in 0.1 M neutral phosphate buffer. (b) UV-visible spectra of 0.05 mM solution of complex 1 (red line) and complex 2 (blue line) in 0.1 M neutral phosphate buffer.	18
22	<b>Fig. S14</b> (a) UV-visible spectra of 1 mM solution of complex 1 in water (red line) and in 0.1 M neutral phosphate buffer (blue line). (b) UV-visible spectra of 0.05 mM solution of complex 1 in water (red line) and in 0.1 M neutral phosphate buffer (blue line)	18
23	<b>Fig. S15</b> (a) UV-visible spectra of 1 mM solution of complex 2 in water (red line) and in 0.1 M neutral phosphate buffer (blue line). (b) UV-visible spectra of 0.05 mM solution of complex 2 in water (red line) and in 0.1 M neutral phosphate buffer (blue line)	19
24	<b>Fig. S16</b> (a) UV-visible spectra of 1 mM solution of complex 1 recorded at different time interval in 0.1 M neutral phosphate buffer. (b) UV-visible spectra of 0.05 mM solution of complex 1 recorded at different time interval in 0.1 M neutral phosphate buffer.	19

25	<b>Fig. S17</b> (a) UV-visible spectra of 1 mM solution of complex 2 recorded at different time interval in 0.1 M neutral phosphate buffer. (b) UV-visible spectra of 0.05 mM solution of complex 2 recorded at different time interval in 0.1 M neutral phosphate buffer.	20
26	<b>Fig. S18</b> UV-visible spectra of (a) 1 mM solution and (b) 0.05 mM solution of complex 3 in 0.1 M neutral phosphate buffer.	20
27	<b>Fig. S19</b> UV-visible spectra of (a) 1 mM solution and (b) 0.05 mM solution of complex 4 in 0.1 M neutral phosphate buffer.	21
28	<b>Fig. S20</b> UV-visible spectra of (a) 1 mM solution and (b) 0.05 mM solution of complex 5 in 0.1 M neutral phosphate buffer.	21
29	<b>Fig. S21</b> UV-visible spectra of (a) 1 mM solution and (b) 0.05 mM solution of complex 6 in 0.1 M neutral phosphate buffer.	22
30	<b>Fig. S22</b> UV-visible spectra of (a) 1 mM solution and (b) 0.05 mM solution of complex 7 in 0.1 M neutral phosphate buffer.	22
31	<b>Fig. S23</b> UV-visible spectra of (a) 1 mM solution and (b) 0.05 mM solution of complex $[\text{Cu}(\text{bipy})_2](\text{ClO}_4)_2$ in 0.1 M neutral phosphate buffer.	23
32	<b>Fig. S24</b> UV-visible spectra of (a) 1 mM solution and (b) 0.05 mM solution of complex $[\text{Cu}(\text{phen})_2](\text{ClO}_4)_2$ in 0.1 M neutral phosphate buffer.	23
33	<b>Fig. S25</b> EPR spectra of (a) Complex 1 and (b) Complex 2 in 0.1 M neutral phosphate buffer.	24
34	<b>Fig. S26</b> Cyclic voltammogram of 1 mM solution of (a) complex 1 and (b) complex 2 in 0.1 M neutral phosphate at $100 \text{ mVs}^{-1}$ scan rate. The onset potentials for water oxidation located near 1.27 V and 1.31 V vs. NHE for complexes 1 and 2, respectively.	24
35	<b>Fig. S27</b> (a) Cyclic voltammograms of complex 1 at 20 (black), 30 (red), 40 (green), 50 (blue), 60 (purple) and 70 (navy) $\text{mVs}^{-1}$ scan rates in 0.1 M neutral phosphate buffer. (b) Plot of $-\ln v$ vs. potential of complex 1 for cathodic current of Cu(II)-Cu(I) couple (red dot), anodic current of Cu(II)-Cu(I) couple (green dot), 2nd anodic peak (blue dot) and 3rd anodic peak (orange dot).	25
36	<b>Fig. S28</b> (a) Cyclic voltammograms of complex 2 at 20 (black), 30 (red), 40 (green), 50 (blue), 60 (purple) and 70 (navy) $\text{mVs}^{-1}$ scan rates in 0.1 M neutral phosphate buffer. (b) Plot of $-\ln v$ vs. potential of complex 2 for cathodic current of Cu(II)-Cu(I) couple (red dot), anodic current of Cu(II)-Cu(I) couple (green dot), 2 <sup>nd</sup> anodic peak (blue dot) and 3 <sup>rd</sup> anodic peak (orange dot).	25
37	<b>Fig. S29</b> (a) Cyclic voltammograms and (b) Differential Pulse voltammograms of complex 1 (blue), and analogous Zn complex, $[\text{Zn}(\text{bipy})(\text{HL}_1)](\text{ClO}_4)_2$ (red) in 0.1 M neutral phosphate buffer recorded with a glassy carbon (GC) working electrode, a Ag/AgCl reference electrode and a Pt counter electrode, scan rate $100 \text{ mVs}^{-1}$ .	26
38	<b>Fig. S30</b> (a) Cyclic voltammograms and (b) Differential Pulse voltammograms of complex 2 (blue), and analogous Zn complex, $[\text{Zn}(\text{phen})(\text{HL}_1)](\text{ClO}_4)_2$ (red) in 0.1 M neutral phosphate buffer recorded with a glassy carbon (GC) working electrode, a Ag/AgCl reference electrode and a Pt counter electrode, scan rate $100 \text{ mVs}^{-1}$ .	26
39	<b>Fig. S31</b> (a) Cyclic voltammograms and (b) Differential Pulse voltammograms of ligand $\text{HL}_1$ , $\text{N}^1$ -(2-aminoethyl)ethane-1,2-diamine (blue), and its $\text{N}^1$ -methylated form, $\text{N}^1$ -(2-aminoethyl)-N1-methylethane-1,2-diamine (red) in 0.1 M neutral phosphate buffer recorded with a glassy carbon (GC)	27

	working electrode, a Ag/AgCl reference electrode and a Pt counter electrode, scan rate 100 mVs <sup>-1</sup> .	
40	<b>Fig. S32</b> UV-visible spectra of (a) complex 1 and (b) complex 2 before electrolysis (blue), and during electrolysis (red) at 1.02 V and 1.01 V vs. NHE respectively in 0.1 M neutral phosphate buffer.	27
41	<b>Fig. S33</b> (a) Cyclic voltammograms of complex 1 at 0.08 (black), 0.16 (red), 0.24 (green), 0.32 (blue), 0.40 (cyan), 0.48 (magenta), 0.56 (navy), 0.64 (purple), 0.72 (royal), 0.80 (orange) and 0.88 mM (violet) concentration in 0.1 M neutral phosphate buffer. Scan rate: 100 mVs <sup>-1</sup> . (b) Catalytic current at 1.32 V vs. NHE for complex 1 as a function of the catalyst concentration from 0.08 mM to 0.88 mM in 0.1 M neutral phosphate buffer.	28
42	<b>Fig. S34</b> (a) Cyclic voltammograms of complex 2 at 0.08 (black), 0.16 (red), 0.24 (green), 0.32 (blue), 0.40 (cyan), 0.48 (magenta), 0.56 (navy), 0.64 (purple), 0.72 (royal), 0.80 (orange) and 0.88 mM (violet) concentration in 0.1 M neutral phosphate buffer. Scan rate: 100 mVs <sup>-1</sup> . (b) Catalytic current at 1.34 V vs. NHE for complex 2 as a function of the catalyst concentration from 0.08 mM to 0.88 mM in 0.1 M neutral phosphate buffer.	28
43	<b>Fig. S35</b> (a) Cyclic voltammograms of complex 1 in the range 0.24 to -0.24 V vs. NHE at 20 (black), 30 (red), 40 (green), 50 (blue), 60 (cyan), 70 (magenta), 80 (navy), 90 (purple) and 100 (royal) mVs <sup>-1</sup> scan rate. (b) Dependence of the peak current for the Cu <sup>II</sup> /Cu <sup>I</sup> couple of complex 1 on the square root of scan rate with standard three electrode system in 0.1 M neutral phosphate buffer. $D_{Cu} = 12.96 \times 10^{-7} \text{ cm}^2/\text{s}$ .	29
44	<b>Fig. S36</b> (a) Cyclic voltammograms of complex 2 in the range 0.36 to -0.12 V vs. NHE at 20 (black), 30 (red), 40 (green), 50 (blue), 60 (cyan), 70 (magenta), 80 (navy), 90 (purple) and 100 (royal) mVs <sup>-1</sup> scan rate. (b) Dependence of the peak current for the Cu <sup>II</sup> /Cu <sup>I</sup> couple of complex 2 on the square root of scan rate with standard three electrode system in 0.1 M neutral phosphate buffer. $D_{Cu} = 11.72 \times 10^{-7} \text{ cm}^2/\text{s}$ .	29
45	<b>Fig. S37</b> (a) Cyclic voltammograms of 0.5 mM solution of complex 1 in 0.1 M (black), 0.075 M (red), 0.05 M (blue) and 0.025 M (green) neutral phosphate buffer at a scan rate of 100 mVs <sup>-1</sup> . (b) Plot of $(i_{cat}/i_d)^2$ vs. different concentration of buffer for 0.5 mM solution of complex 1.	30
46	<b>Fig. S38</b> (a) Cyclic voltammograms of 0.5 mM solution of complex 2 in 0.1 M (black), 0.075 M (red), 0.05 M (blue) and 0.025 M (green) neutral phosphate buffer at a scan rate of 100 mVs <sup>-1</sup> . (b) Plot of $(i_{cat}/i_d)^2$ vs. different concentration of buffer for 0.5 mM solution of complex 2.	30
47	<b>Fig. S39</b> (a) Cyclic voltammograms of complex 1 with currents normalized to the square root of the scan rates 30 (black), 40 (red), 50 (green) and 70 (blue) mVs <sup>-1</sup> measured in 0.1 M neutral phosphate buffer. (b) Cyclic voltammograms of complex 2 with currents normalized to the square root of the scan rates 20 (black), 30 (red), 60 (green), 70 (blue) and 90 (purple) mVs <sup>-1</sup> measured in 0.1 M neutral phosphate buffer	31
48	<b>Fig. S40</b> Cyclic voltammograms of (a) complex 1 and (b) complex 2 in H <sub>2</sub> O (Red) and D <sub>2</sub> O (Black) 0.1 M phosphate buffer recorded with a glassy carbon (GC) working electrode, a Ag/AgCl reference electrode and a Pt counter electrode. Scan rate, 100 mVs <sup>-1</sup> .	31
49	<b>Fig. S41</b> Cyclic voltammograms (7 sweeps) of complex 3 recorded in 0.1 M neutral phosphate buffer at scan rate 100 mVs <sup>-1</sup> . Black line corresponds to	32

	sweeps 1-3, red line for sweeps 4-5 and blue line for sweeps 6-7.	
50	<b>Fig. S42</b> Cyclic voltammograms of complex 3 recorded before (blue) and after (red) bulk electrolysis at 1.35 V vs. NHE in 0.1 M neutral phosphate buffer using glassy carbon (GC) as working electrode (area 0.07 cm <sup>2</sup> ), Ag/AgCl as reference electrode and Pt as counter electrode. Scan rate, 100 mVs <sup>-1</sup> .	32
51	<b>Fig. S43</b> FE-SEM and EDX plot of (a) fresh ITO working electrode (b) ITO working electrode after bulk electrolysis of complex 3 in 0.1 M neutral phosphate buffer.	33
52	<b>Fig. S44</b> (a) Cyclic voltammogram of 1 mM solution of complex [Cu(bipy) <sub>2</sub> ](ClO <sub>4</sub> ) <sub>2</sub> (blue line) in 0.1 M neutral phosphate buffer at a scan rate of 100 mVs <sup>-1</sup> . The red line indicates the cyclic voltammogram of 0.1 M neutral phosphate buffer in absence of complex at a scan rate of 100 mVs <sup>-1</sup> .(b) Differential pulse voltammogram of 1 mM solution of complex [Cu(bipy) <sub>2</sub> ](ClO <sub>4</sub> ) <sub>2</sub> (blue line) in 0.1 M neutral phosphate buffer. The red line indicates the differential pulse voltammogram of 0.1 M neutral phosphate buffer in absence of complex.	33
53	<b>Fig. S45</b> (a) Cyclic voltammogram of 1 mM solution of complex [Cu(phen) <sub>2</sub> ](ClO <sub>4</sub> ) <sub>2</sub> (blue line) in 0.1 M neutral phosphate buffer at a scan rate of 100 mVs <sup>-1</sup> . The red line indicates the cyclic voltammogram of 0.1 M neutral phosphate buffer in absence of complex at a scan rate of 100 mVs <sup>-1</sup> .(b) Differential pulse voltammogram of 1 mM solution of complex [Cu(phen) <sub>2</sub> ](ClO <sub>4</sub> ) <sub>2</sub> (blue line) in 0.1 M neutral phosphate buffer. The red line indicates the differential pulse voltammogram of 0.1 M neutral phosphate buffer in absence of complex.	34
54	<b>Fig. S46</b> (a) Cyclic voltammograms and (b) Differential Pulse voltammograms of ligands HL <sub>1</sub> , N <sup>1</sup> -(2-aminoethyl)ethane-1,2-diamine (blue), HL <sub>2</sub> , bis(pyridin-2-ylmethyl)amine (red) and L <sub>3</sub> , 2,6-di(pyridin-2-yl)pyridine (black) in 0.1 M neutral phosphate buffer recorded with a glassy carbon (GC) working electrode, a Ag/AgCl reference electrode and a Pt counter electrode, scan rate 100 mVs <sup>-1</sup> .	34
55	<b>Fig. S47</b> (a) Cyclic voltammogram of 1 mM solution of complex 4 (blue line) in 0.1 M neutral phosphate buffer at a scan rate of 100 mVs <sup>-1</sup> . The red line indicates the cyclic voltammogram of 0.1 M neutral phosphate buffer in absence of complex at a scan rate of 100 mVs <sup>-1</sup> .(b) Differential pulse voltammogram of 1 mM solution of complex 4 (blue line) in 0.1 M neutral phosphate buffer. The red line indicates the differential pulse voltammogram of 0.1 M neutral phosphate buffer in absence of complex.	35
56	<b>Fig. S48</b> (a) Cyclic voltammogram of 1 mM solution of complex 5 (blue line) in 0.1 M neutral phosphate buffer at a scan rate of 100 mVs <sup>-1</sup> . The red line indicates the cyclic voltammogram of 0.1 M neutral phosphate buffer in absence of complex at a scan rate of 100 mVs <sup>-1</sup> .(b) Differential pulse voltammogram of 1 mM solution of complex 5 (blue line) in 0.1 M neutral phosphate buffer. The red line indicates the differential pulse voltammogram of 0.1 M neutral phosphate buffer in absence of complex.	35
57	<b>Fig. S49</b> (a) Cyclic voltammogram of 1 mM solution of complex 6 (blue line) in 0.1 M neutral phosphate buffer at a scan rate of 100 mVs <sup>-1</sup> . The red line indicates the cyclic voltammogram of 0.1 M neutral phosphate buffer in absence of complex at a scan rate of 100 mVs <sup>-1</sup> .(b) Differential pulse	36

	voltammogram of 1 mM solution of complex 6 (blue line) in 0.1 M neutral phosphate buffer. The red line indicates the differential pulse voltammogram of 0.1 M neutral phosphate buffer in absence of complex.	
58	<b>Fig. S50</b> (a) Cyclic voltammogram of 1 mM solution of complex 7 (blue line) in 0.1 M neutral phosphate buffer at a scan rate of 100 mVs <sup>-1</sup> . The red line indicates the cyclic voltammogram of 0.1 M neutral phosphate buffer in absence of complex at a scan rate of 100 mVs <sup>-1</sup> .(b) Differential pulse voltammogram of 1 mM solution of complex 7 (blue line) in 0.1 M neutral phosphate buffer. The red line indicates the differential pulse voltammogram of 0.1 M neutral phosphate buffer in absence of complex.	36
59	<b>Fig. S51</b> Cyclic voltammogram of 1 mM solution of (a) complex 4 and (b) complex 5 in 0.1 M neutral phosphate at 100 mVs <sup>-1</sup> scan rate. The onset potentials for water oxidation located near 1.72 V and 1.73 V vs. NHE for complexes 4 and 5 respectively.	37
60	<b>Fig. S52</b> (a) Cyclic voltammograms of complex 4 at 4 (black), 6 (red), 8 (green), 10 (blue), 12 (purple) and 14 (violet) mVs-1 scan rates in 0.1 M neutral phosphate buffer. (b) Plot of $i_{cat}/i_d$ vs. $v^{-1/2}$ at each scan rate for complex 4.	37
61	<b>Fig. S53</b> (a) Cyclic voltammograms of complex 5 at 4 (black), 6 (red), 8 (green), 10 (blue), 12 (purple) and 14 (violet) mVs-1 scan rates in 0.1 M neutral phosphate buffer. (b) Plot of $i_{cat}/i_d$ vs. $v^{-1/2}$ at each scan rate for complex 5.	38
62	<b>Fig. S54</b> Plot of current density vs. time recorded during 4 hour of bulk electrolysis with (blue line) and without (red line) (a) complex 1 and (b) complex 2 in 0.1 M neutral phosphate buffer using ITO working electrode (area 4 cm <sup>2</sup> ), Ag/AgCl reference electrode and Pt counter electrode at 1.32 V vs. NHE and 1.34 V vs. NHE respectively.	38
63	<b>Fig. S55</b> Plot of current density vs. time recorded during 4 hour of bulk electrolysis with (blue line) and without (red line) (a) complex 4 and (b) complex 5 in 0.1 M neutral phosphate buffer using ITO working electrode (area 4 cm <sup>2</sup> ), Ag/AgCl reference electrode and Pt counter electrode at 1.73 V vs. NHE and 1.75 V vs. NHE respectively.	39
64	<b>Fig. S56</b> Oxygen evolution during the bulk electrolysis with an ITO electrode (area = 4 cm <sup>2</sup> ) for (a) complex 4 and (b) complex 5 at 1.73 and 1.75 V vs. NHE respectively for 4 hour with (blue line) and without copper complexes (red line). The black line indicates the theoretical amount of oxygen as assumed by charge passed with 100 % faradic efficiency.	39
65	<b>Fig. S57</b> Cyclic voltammograms of (a) complex 1 and (b) complex 2 recorded before (red) and after (blue) 4 hour of bulk electrolysis at 1.32 V and 1.34 V vs. NHE respectively in 0.1 M neutral phosphate buffer using glassy carbon (GC) as working electrode (area 0.07 cm <sup>2</sup> ), Ag/AgCl as reference electrode and Pt as counter electrode. Scan rate, 100 mVs <sup>-1</sup> .	40
66	<b>Fig. S58</b> Cyclic voltammograms of (a) complex 4 and (b) complex 5 recorded before (blue) and after (red) 4 hour of bulk electrolysis at 1.73 V and 1.75 V vs. NHE respectively in 0.1 M neutral phosphate buffer using glassy carbon (GC) as working electrode (area 0.07 cm <sup>2</sup> ), Ag/AgCl as reference electrode and Pt as counter electrode. Scan rate, 100 mVs <sup>-1</sup> .	40
67	<b>Fig. S59</b> UV-visible spectra of (a) complex 1 and (b) complex 2 recorded before (red) and after (blue) 4 hour of bulk electrolysis at 1.32 V and 1.34 V vs. NHE respectively in 0.1 M neutral phosphate buffer.	41
68	<b>Fig. S60</b> UV-visible spectra of (a) complex 4 and (b) complex 5 recorded	41

	before (blue) and after (red) 4 hour of bulk electrolysis at 1.73 V and 1.75 V vs. NHE respectively in 0.1 M neutral phosphate buffer.	
<b>69</b>	<b>Fig. S61</b> Cyclic voltammograms recorded in 0.1 M neutral phosphate buffer in the absence of (a) complex 1 and (b) complex 2 with fresh (red) and used (blue) ITO working electrode (area 4 cm <sup>2</sup> ), a Ag/AgCl reference electrode and a Pt counter electrode, scan rate. 100 mVs <sup>-1</sup> .	<b>42</b>
<b>70</b>	<b>Fig. S62</b> Cyclic voltammograms recorded in 0.1 M neutral phosphate buffer in the absence of (a) complex 4 and (b) complex 5 with fresh (blue) and used (red) ITO working electrode (area 4 cm <sup>2</sup> ), a Ag/AgCl reference electrode and a Pt counter electrode, scan rate, 100 mVs <sup>-1</sup> .	<b>42</b>
<b>71</b>	<b>Fig. S63</b> FE-SEM and EDX plot of (a) fresh ITO working electrode (b) ITO working electrode after 4 hour of bulk electrolysis of complex 1 and (c) ITO working electrode after 4 hour of bulk electrolysis of complex 2 in 0.1 M neutral phosphate buffer.	<b>43</b>
<b>72</b>	<b>Fig. S64</b> FE-SEM and EDX plot of (a) fresh ITO working electrode (b) ITO working electrode after 4 hour of bulk electrolysis of complex 4 and (c) ITO working electrode after 4 hour of bulk electrolysis of complex 5 in 0.1 M neutral phosphate buffer.	<b>44</b>
<b>73</b>	<b>Fig. S65</b> (a) Plot of charge vs. time recorded during bulk electrolysis of complex 4 at 0.0 mM (black), 0.1 mM (red), 0.2 mM (green), 0.3 mM (blue), 0.4 mM (purple) and 0.5 mM (violet) concentration at 1.73 V vs. NHE. (b) Plot of total charge vs. concentration of complex 4 after 1 hour of electrolysis.	<b>45</b>
<b>74</b>	<b>Fig. S66</b> (a) Plot of charge vs. time recorded during bulk electrolysis of complex 5 at 0.0 mM (black), 0.1 mM (red), 0.2 mM (green), 0.3 mM (blue), 0.4 mM (purple) and 0.5 mM (violet) concentration at 1.75 V vs. NHE. (b) Plot of total charge vs. concentration of complex 5 after 1 hour of electrolysis.	<b>45</b>
<b>75</b>	<b>Table S1</b> Crystal data and structure refinement parameters for Complexes 1 and 2	<b>46</b>
<b>76</b>	<b>Table S2</b> Crystal data and structure refinement parameters for Complexes 3 and 4	<b>47</b>
<b>77</b>	<b>Table S3</b> Crystal data and structure refinement parameters for Complexes 5 and 6	<b>48</b>
<b>78</b>	<b>Table S4</b> Crystal data and structure refinement parameters for Complexes [Zn(bipy)(HL <sub>1</sub> )](ClO <sub>4</sub> ) <sub>2</sub> and [Zn(phen)(HL <sub>1</sub> )](ClO <sub>4</sub> ) <sub>2</sub>	<b>49</b>
<b>79</b>	References:	<b>50</b>

## Experimental Procedures:

All reagents and solvents were purchased from commercial sources and were of reagent grade. UV-visible spectra were recorded on Cary-60 UV-Visible spectrophotometer. FT-IR spectra were recorded on a Cary 630 spectrophotometer with sample prepared as KBr pellets. The magnetic moment of the complex were measured on a Cambridge magnetic balance. Conductivity measurements were recorded using a Eutech instrument CON 700. Elemental analyses were carried out on a Thermo Scientific Flashmart Analyzer. Electrochemical measurements were made using CHI 7035E bipotentiostat. Glassy carbon working electrode, Pt wire auxiliary electrode, and Ag/AgCl reference electrode were used in a three-electrode configuration. A Carl Zeiss Supra 55 electron microscope was used for Field Emission Scanning Electron Microscope (FE-SEM) studies after Au coating. A 20 kV electron beam used for collection of EDX spectra and atomic mapping images. Powder X-ray diffraction (PXRD) data were collected from 5 to 50<sup>0</sup> 2 $\theta$  using a Bruker-D8 Advance X-ray diffractometer.

The single crystal data were collected on a Bruker Smart Apex Duo diffractometer, utilizing MoK $\alpha$  radiation ( $\lambda = 0.71073 \text{ \AA}$ ). The structures were initially solved with the direct method and further refined by employing full-matrix least squares based on F<sup>2</sup>, using SHELXL-2014/7 software integrated into Apex 3 suite.<sup>S1</sup> All the hydrogen positions were initially located in the difference Fourier maps, and for the final refinement, the hydrogen atoms were placed in geometrically ideal positions and refined in the riding mode.<sup>S2</sup> Final refinement included atomic positions for all the atoms, anisotropic thermal parameters for all the non-hydrogen atoms, and isotropic thermal parameters for all the hydrogen atoms were carried out using Olex2 1.2 package of programs.<sup>S3,S4</sup> Structural illustrations have been drawn with ORTEP-3 for Windows. CCDC: 2401171, 2401172, 2435313, 2435314, 2435315, 2435316, 2435317, and 2435318 contains the crystallographic data for this paper. These data can be obtained free of charge from The Cambridge Crystallographic Data Centre (CCDC) via [www.ccdc.cam.ac.uk/data\\_request/cif](http://www.ccdc.cam.ac.uk/data_request/cif).

### Electron count in redox peak using Laviron equations:

To obtain the number of electrons transferred in a redox peak, Laviron equations are used. The Laviron equations are given as below.

$$E_{p,c} = E^{\ominus} - (RT/\alpha nF) \ln(\alpha n\nu/RTk) = C - (RT/\alpha nF) \ln(\nu) \quad (1)$$

$$E_{p,a} = E^{\ominus} + [RT/(1-\alpha)nF] \ln[(1-\alpha)n\nu/RTk] = C + [RT/(1-\alpha)nF] \ln(\nu) \quad (2)$$

$$E_{p/2} = C + [RT/(1-\alpha)nF] \ln(\nu) \quad (3)$$

Where,  $E^{\ominus}$  is the standard potential,  $E_{p,c}$  is the potential for cathodic peak,  $E_{p,a}$  is the potential for anodic peak, R is the ideal gas constant, T is temperature, F is Faraday constant,  $k$  is the rate constant of the electrochemical reaction ( $s^{-1}$ ) and C is the constant.

The  $\alpha$  value is calculated using equation (1) and equation (2) for a reversible couple from the slope of  $E_{p,a}$  vs.  $-\ln \nu$  and  $E_{p,c}$  vs.  $-\ln \nu$ . With the calculated value of  $\alpha$ , number of electron ( $n$ ) can be calculated. For the irreversible peak, number of electron ( $n$ ) can be calculated using equation (3) from the slope of  $E_{1/2}$  vs.  $-\ln \nu$ . The value of  $E_{p,a}$ ,  $E_{p,c}$  and  $E_{1/2}$  are obtained from the cyclic voltammograms of the complexes at different scan rates.

### Calculation of Faradic efficiency:

$$\% \text{ Faradic efficiency} = [(\text{Actual amount of oxygen produced}) / (\text{Theoretically calculated amount of oxygen})] \times 100$$

The theoretically calculated amount of oxygen during Bulk Electrolysis (BE) experiment can be obtained using the following relation:

$$\text{Theoretical yield of oxygen (in mol L}^{-1}\text{)} = (Q / 4FV)$$

Where,

Q = Total charge passed during Bulk Electrolysis (BE) experiment in coulomb.

F = Faraday constant

V = Volume of the complex solution used for bulk electrolysis (BE) experiment in Litter

### Synthesis of [Cu(bipy)<sub>2</sub>](ClO<sub>4</sub>)<sub>2</sub>

2,2'-bipyridine (bipy) (0.50 g, 3.2 mmol) was dissolved in 10 mL methanol. To this solution Copper (II) perchlorate hexahydrate, [Cu(H<sub>2</sub>O)<sub>6</sub>](ClO<sub>4</sub>)<sub>2</sub> (0.59 g, 1.6 mmol) dissolved in 10 ml methanol was added drop wise which results appearance of blue colour precipitate. After 1 hour, the resulting mixture was filtered and the precipitate was dissolved in methanol-water mixture and kept for crystallization at room temperature which results blue crystalline compounds. Yield: 0.97 g (~88%). Elemental Analyses: Calcd. for C<sub>20</sub>H<sub>16</sub>N<sub>4</sub>Cl<sub>2</sub>O<sub>8</sub>Cu: C, 41.79; H, 2.89; N, 9.75. Found (%): C, 41.77; H, 2.86; N, 9.78. FT-IR (KBr): 3438, 2909, 1612, 1448, 1082 cm<sup>-1</sup>. Molar conductance: 207 Scm<sup>2</sup>mol<sup>-1</sup> (acetonitrile). The observed magnetic moment is found to be 1.68 μB.

### Synthesis of [Cu(Phen)<sub>2</sub>](ClO<sub>4</sub>)<sub>2</sub>

1,10-phenanthroline (phen) (0.50 g, 2.5 mmol) was dissolved in 10 mL methanol. To this solution Copper (II) perchlorate hexahydrate, [Cu(H<sub>2</sub>O)<sub>6</sub>](ClO<sub>4</sub>)<sub>2</sub> (0.47 g, 1.25 mmol) dissolved in 10 ml methanol was added drop wise which results appearance of blue colour precipitate. After 1 hour, the resulting mixture was filtered and the precipitate was dissolved in methanol-water mixture and kept for crystallization at room temperature which results blue crystalline compounds. Yield: 1.05 g (~90%). Elemental Analyses: Calcd. for C<sub>24</sub>H<sub>16</sub>N<sub>4</sub>Cl<sub>2</sub>O<sub>8</sub>Cu: C, 46.28; H, 2.59; N, 9.00. Found (%): C, 46.30; H, 2.56; N, 8.98. FT-IR (KBr): 3451, 2915, 1523, 1421, 1096 cm<sup>-1</sup>. Molar conductance: 206 Scm<sup>2</sup>mol<sup>-1</sup> (acetonitrile). The observed magnetic moment is found to be 1.69 μB.

### Synthesis of [Zn(bipy)(HL<sub>1</sub>)](ClO<sub>4</sub>)<sub>2</sub>

2,2'-bipyridine (bipy) (0.50 g, 3.2 mmol) dissolved in 10 mL methanol and to this solution N<sup>1</sup>-(2-aminoethyl)ethane-1,2-diamine (HL<sub>1</sub>) (0.33g, 3.2 mmol) was dissolved in 10 mL of methanol was added. To the resulting solution, Zinc (II) perchlorate hexahydrate, [Zn(H<sub>2</sub>O)<sub>6</sub>](ClO<sub>4</sub>)<sub>2</sub> (1.19 g, 3.2 mmol) dissolved in 15 ml methanol was added drop wise which results appearance of white precipitate. After 1 hour, the resulting mixture was filtered and the precipitate was dissolved in methanol-water mixture and kept for crystallization at room temperature which results colourless crystalline compounds. Yield: 1.16 g (~93%). Elemental Analyses: Calcd. for

C<sub>14</sub>H<sub>21</sub>N<sub>5</sub>Cl<sub>2</sub>O<sub>8</sub>Zn: C, 32.11; H, 4.04; N, 13.37. Found (%): C, 32.13; H, 4.04; N, 13.35. FT-IR (KBr): 3275, 3180, 2922, 1605, 1428, 1143, 1109, 1082 cm<sup>-1</sup>.

### Synthesis of [Zn(phen)(HL<sub>1</sub>)](ClO<sub>4</sub>)<sub>2</sub>

1,10-phenanthroline (phen) (0.50 g, 2.5 mmol) dissolved in 10 mL methanol and to this solution N<sup>1</sup>-(2-aminoethyl)ethane-1,2-diamine (HL<sub>1</sub>) (0.26g, 2.5 mmol) was dissolved in 10 mL of methanol was added. To the resulting solution, Zinc (II) perchlorate hexahydrate, [Zn(H<sub>2</sub>O)<sub>6</sub>](ClO<sub>4</sub>)<sub>2</sub> (0.94g, 2.5mmol) dissolved in 15 mL methanol was added drop wise which results appearance of white precipitate. After 1 hour, the resulting mixture was filtered and the precipitate was dissolved in methanol-water mixture and kept for crystallization at room temperature which results colourless crystalline compounds. Yield: 1.20 g (~92%). Elemental Analyses: Calcd. for C<sub>16</sub>H<sub>21</sub>N<sub>5</sub>Cl<sub>2</sub>O<sub>8</sub>Zn: C, 35.09; H, 3.87; N, 12.79. Found (%): C, 35.11; H, 3.84; N, 12.81. FT-IR (KBr): 3424, 3207, 2929, 1585, 1517, 1428, 1150, 1068 cm<sup>-1</sup>.

### Controlled potential electrolysis of complexes 4 and 5

To measure Faradaic efficiency of the catalytic reactions, oxygen evolution was investigated through controlled potential electrolysis (CPE) at 1.73 and 1.75 V vs. NHE for complexes 4 and 5 respectively using a large surface-area ITO working electrode (4 cm<sup>2</sup>) in a gas-tight cell (**Fig. S55**). Oxygen formed in the solution was measured using a calibrated Ocean Optics FOXY probe. Faradaic efficiency close to 87% and 82% (**Fig. S56**) were estimated for complexes 4 and 5 respectively during 4 hour of bulk electrolysis experiment. Cyclic voltammograms and UV-visible spectra of the complexes recorded before and after the bulk electrolysis experiment were almost identical (**Fig. S58 and S60**). Cyclic voltammograms recorded with the ITO working electrode before and after bulk electrolysis experiment in the absence of catalyst were essentially identical (**Fig. S62**). FE-SEM and EDX data of fresh and used ITO working electrode shows no evidence of deposition of the electroactive species on the working electrode surface during long term electrolysis experiment for the complexes 4 and 5 (**Fig. S64**). The total charge passed after 1 h of electrolysis under the same conditions varied linearly with the initial concentration of complexes (**Fig. S65 and S66**) with no evidence of an induction period at an early stage of electrolysis, providing evidence for homogeneous single site water oxidation catalysis.

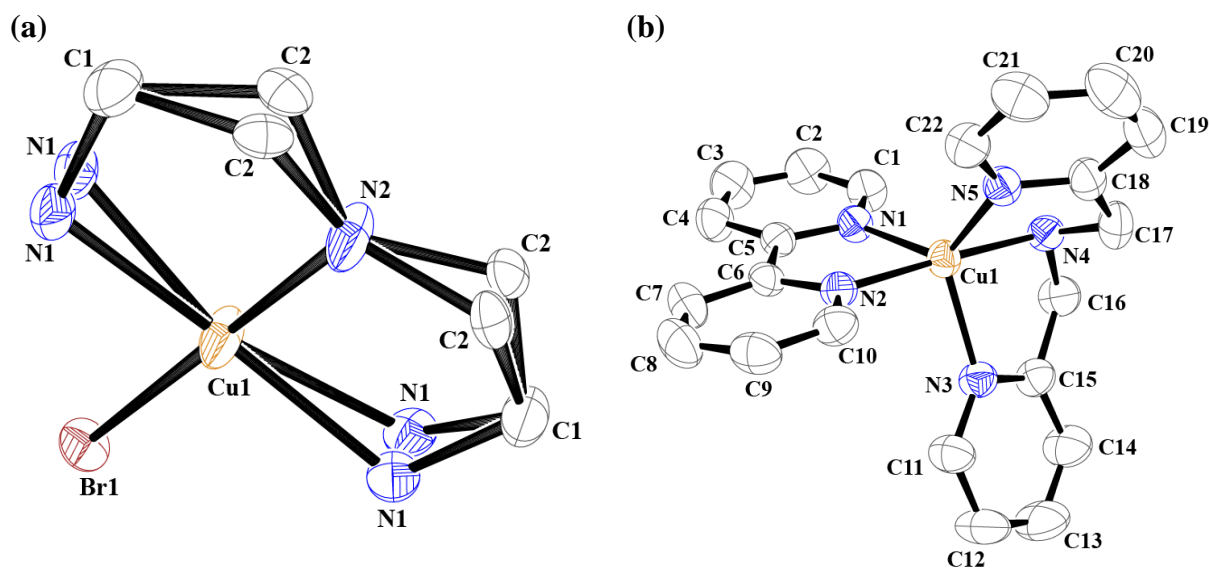


**Fig. S1** ORTEP diagram (50% thermal ellipsoid plot) of (a) complex 3 [the N1 and C2 atoms are modelled as disordered] and (b) complex 4. Counter ions, hydrogen atoms and solvent molecules are removed for clarity.

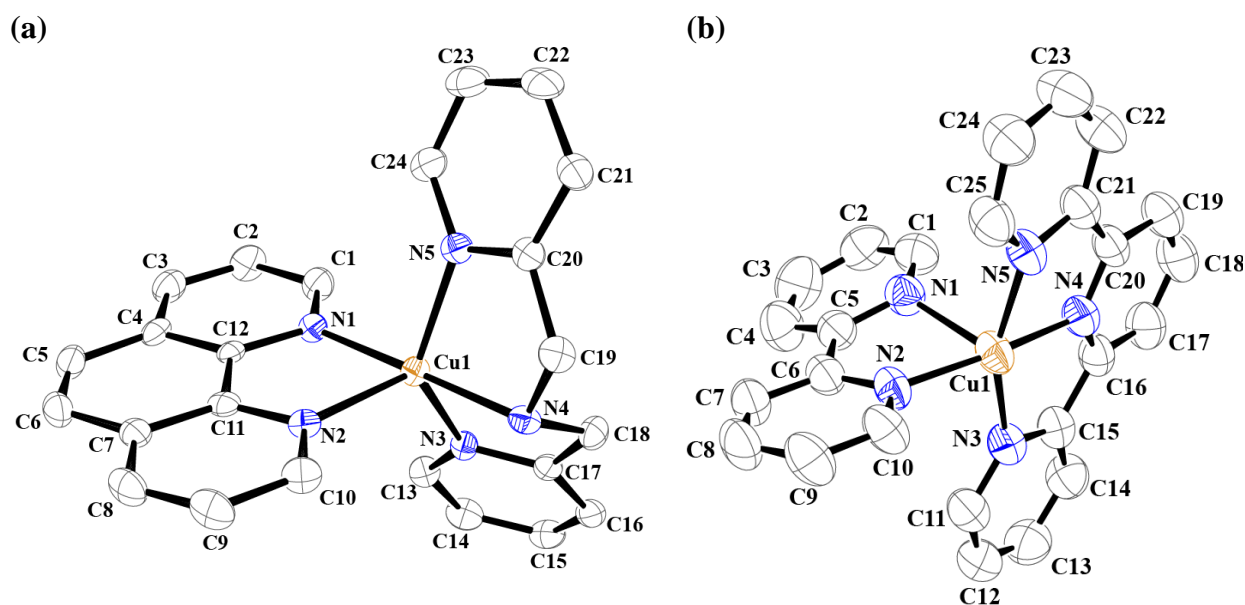


**Fig. S2** ORTEP diagram (50% thermal ellipsoid plot) of (a) complex 5 and (b) complex 6. Counter ions, hydrogen atoms and solvent molecules are removed for clarity.

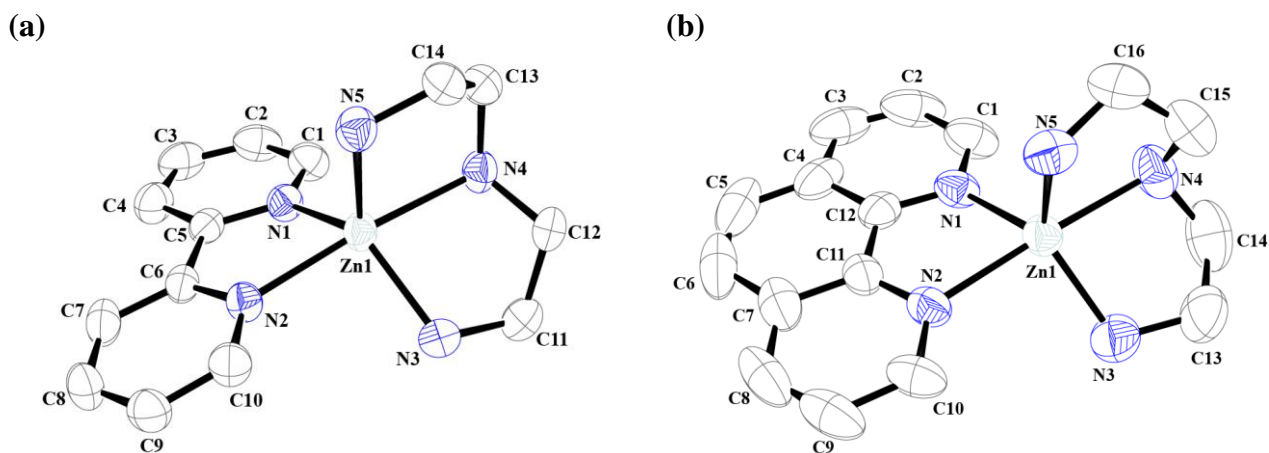


**Fig. S3** ORTEP diagram (50% thermal ellipsoid plot) of (a) complex  $[\text{Zn}(\text{bipy})(\text{HL}_1)](\text{ClO}_4)_2$  and (b) complex  $[\text{Zn}(\text{phen})(\text{HL}_1)](\text{ClO}_4)_2$ . Counter ions, hydrogen atoms and solvent molecules are removed for clarity.

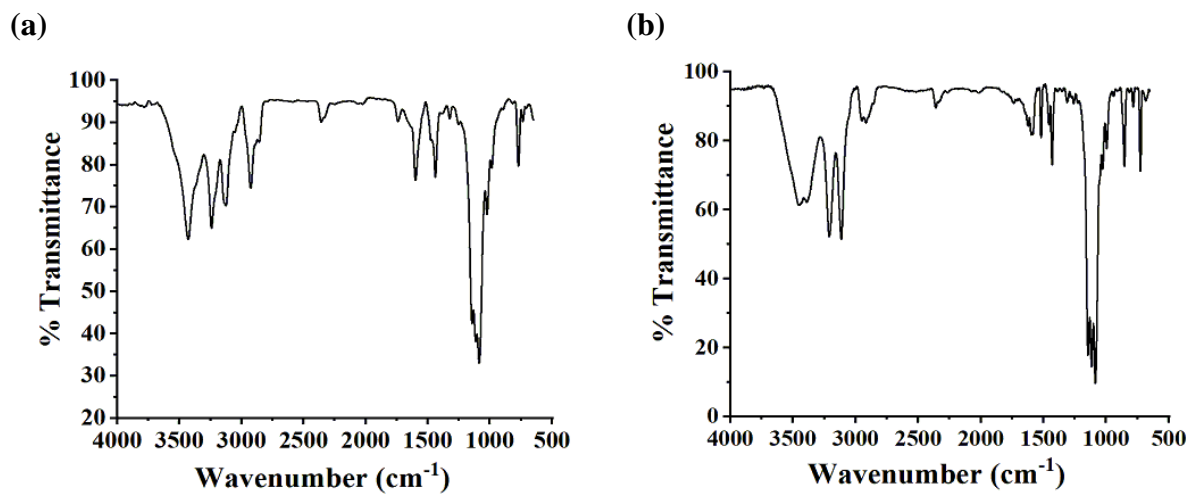


**Fig. S4** FT-IR spectra of (a) complex **1** and (b) complex **2** in KBr.

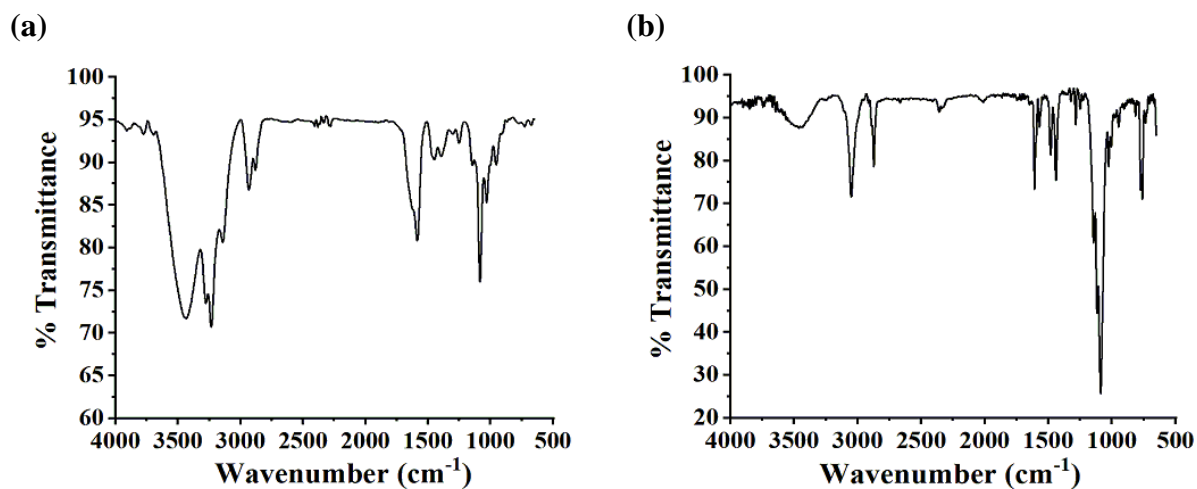


**Fig. S5** FT-IR spectra of (a) complex 3 and (b) complex 4 in KBr.

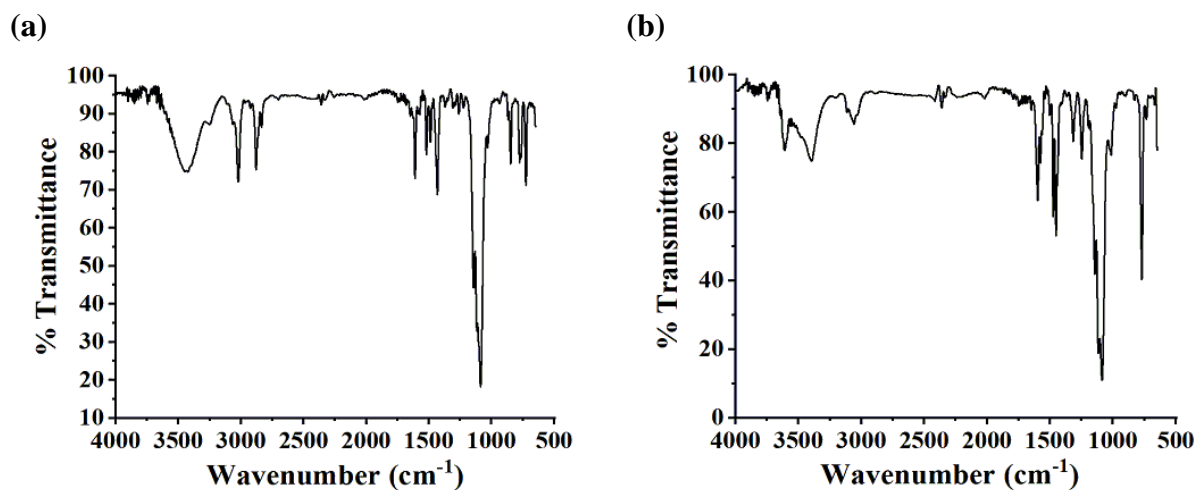


**Fig. S6** FT-IR spectra of (a) complex 5 and (b) complex 6 in KBr.

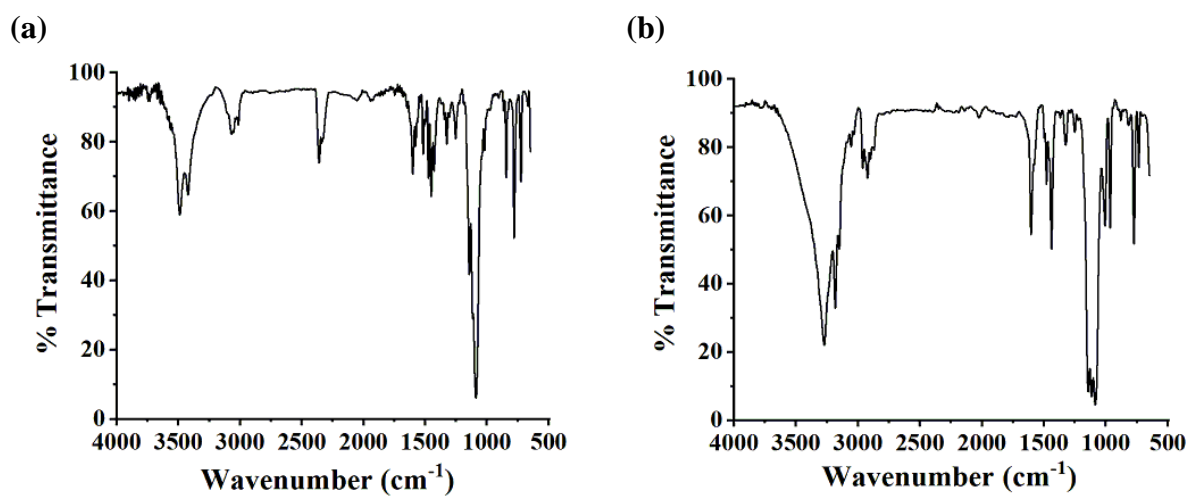


**Fig. S7** FT-IR spectra of (a) complex **7** and (b) complex  $[\text{Zn}(\text{bipy})(\text{HL}_1)](\text{ClO}_4)_2$  in KBr.

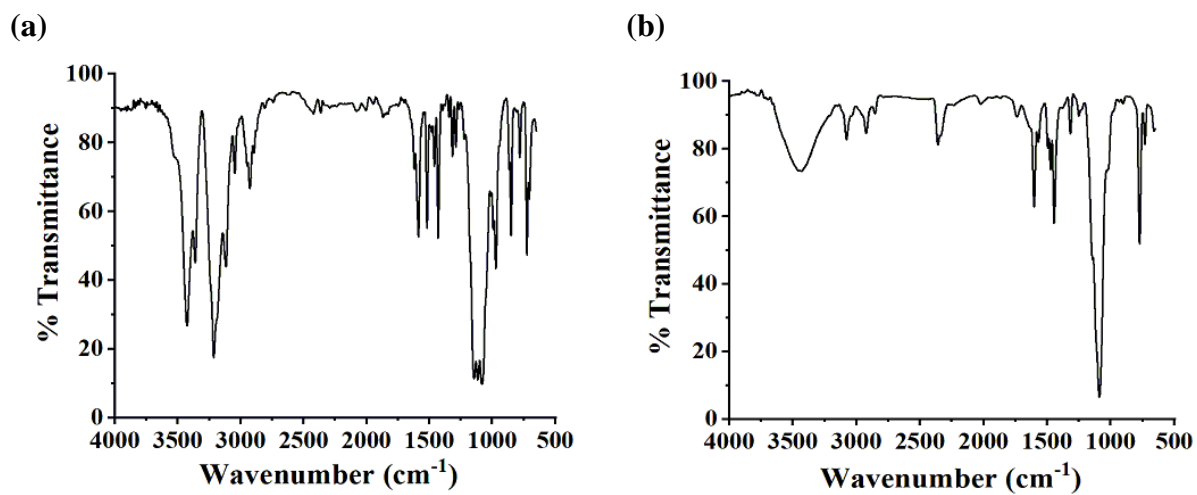


**Fig. S8** FT-IR spectra of (a) complex  $[\text{Zn}(\text{phen})(\text{HL}_1)](\text{ClO}_4)_2$  and (b) complex  $[\text{Cu}(\text{bipy})_2](\text{ClO}_4)_2$  in KBr.

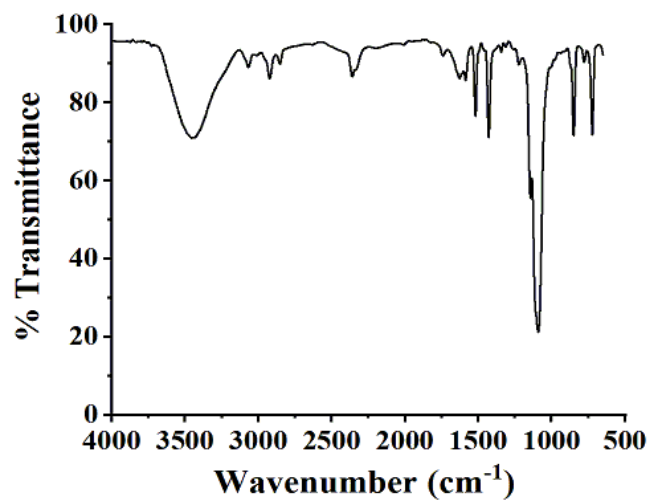


**Fig. S9** FT-IR spectrum of complex  $[\text{Cu}(\text{phen})_2](\text{ClO}_4)_2$  in KBr.

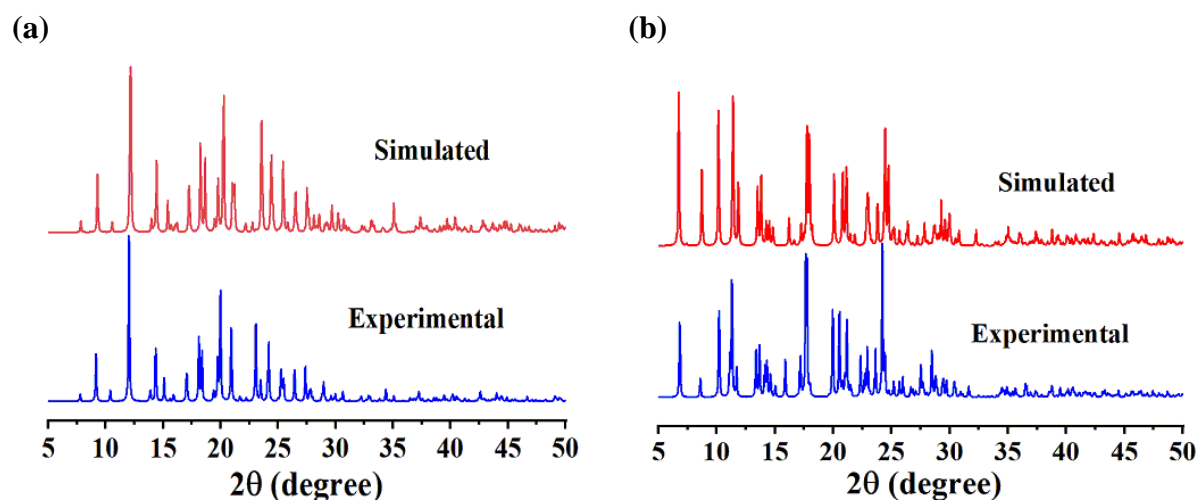


**Fig. S10** PXRD patterns of (a) complex 1 and (b) complex 2.

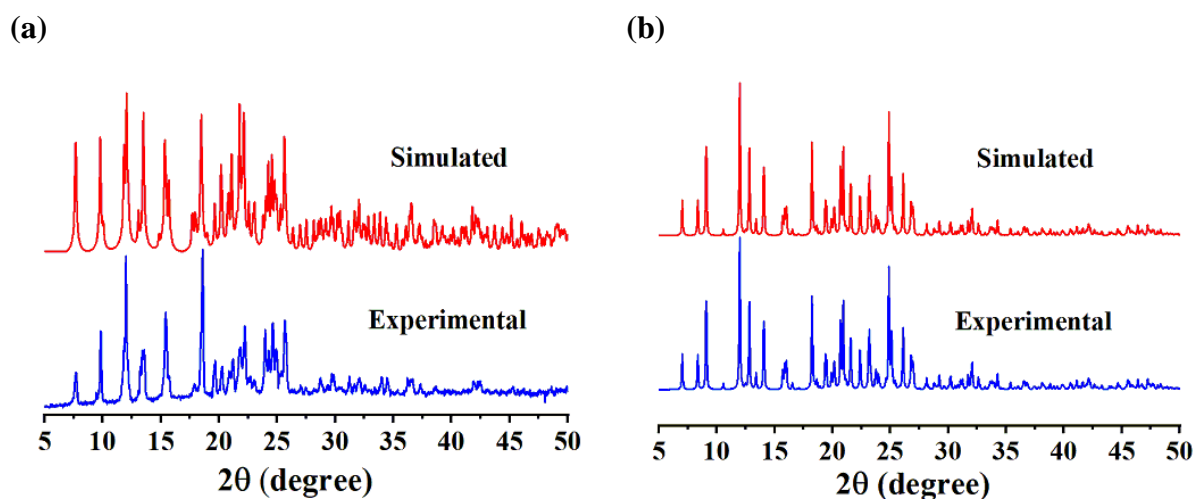


**Fig. S11** PXRD patterns of (a) complex 4 and (b) complex 5.

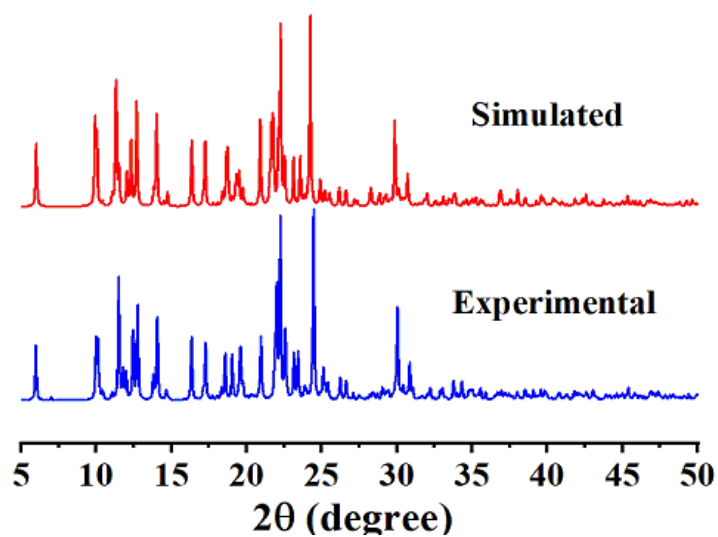


**Fig. S12** PXRD patterns of complex 6.

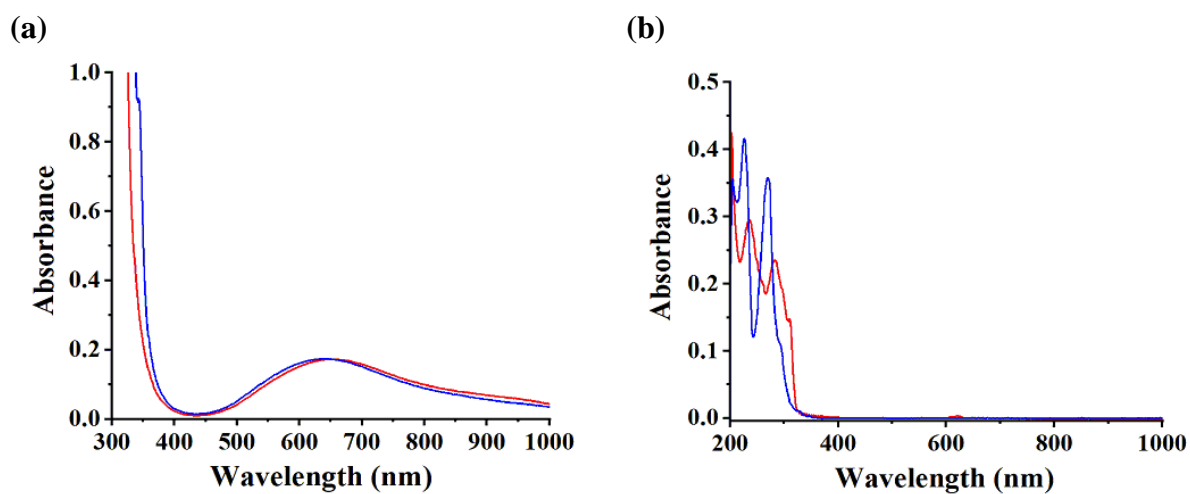


**Fig. S13** (a) UV-visible spectra of 1 mM solution of complex **1** (red line) and complex **2** (blue line) in 0.1 M neutral phosphate buffer. (b) UV-visible spectra of 0.05 mM solution of complex **1** (red line) and complex **2** (blue line) in 0.1 M neutral phosphate buffer.

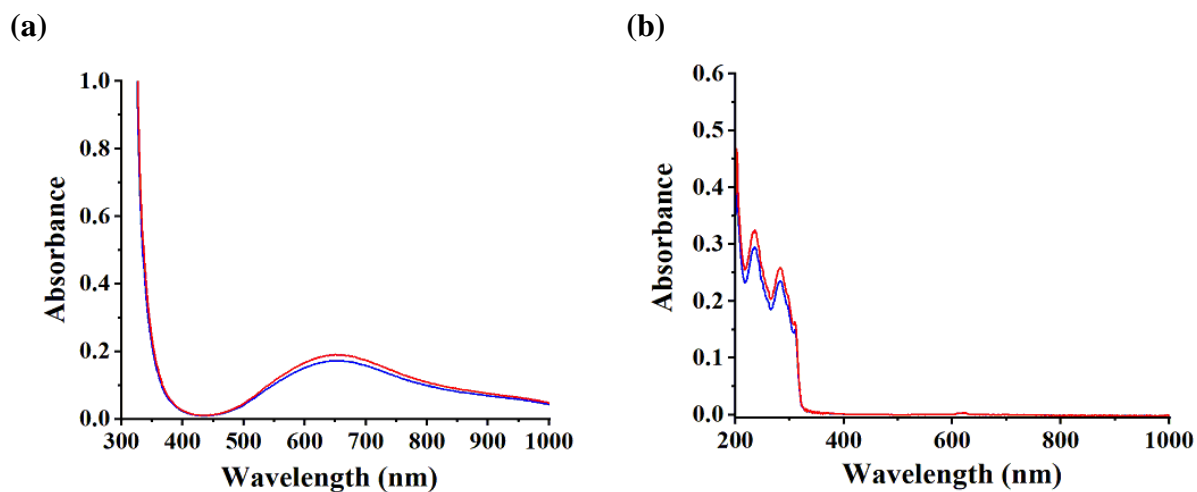


**Fig. S14** (a) UV-visible spectra of 1 mM solution of complex **1** in water (red line) and in 0.1 M neutral phosphate buffer (blue line). (b) UV-visible spectra of 0.05 mM solution of complex **1** in water (red line) and in 0.1 M neutral phosphate buffer (blue line)

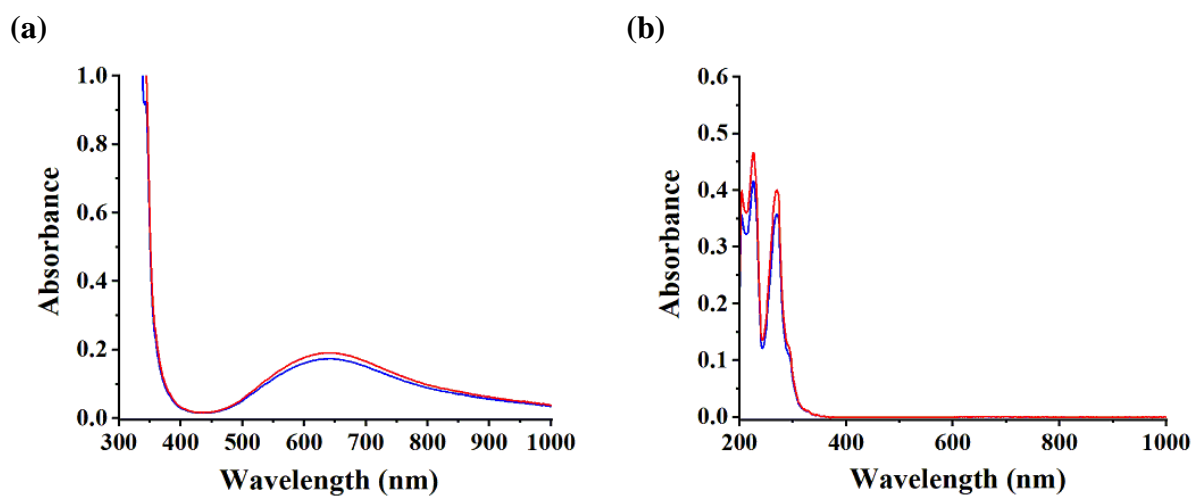


**Fig. S15** (a) UV-visible spectra of 1 mM solution of complex **2** in water (red line) and in 0.1 M neutral phosphate buffer (blue line). (b) UV-visible spectra of 0.05 mM solution of complex **2** in water (red line) and in 0.1 M neutral phosphate buffer (blue line)

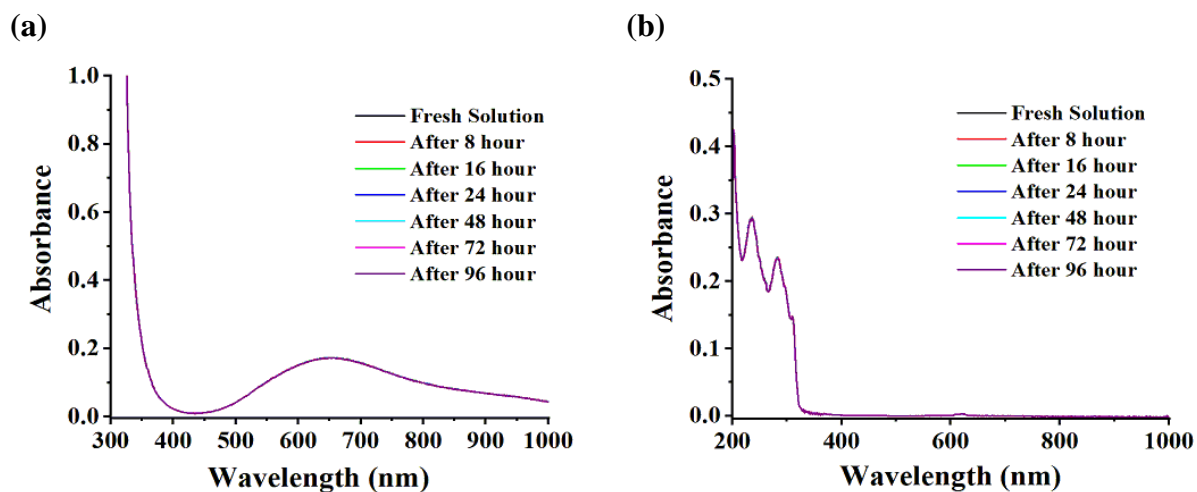


**Fig. S16** (a) UV-visible spectra of 1 mM solution of complex **1** recorded at different time interval in 0.1 M neutral phosphate buffer. (b) UV-visible spectra of 0.05 mM solution of complex **1** recorded at different time interval in 0.1 M neutral phosphate buffer.

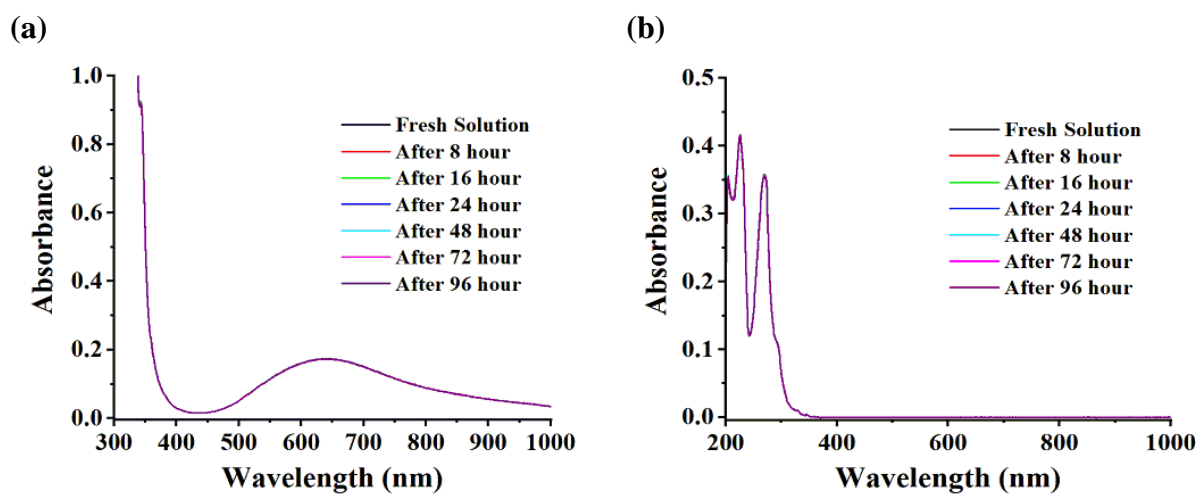


**Fig. S17** (a) UV-visible spectra of 1 mM solution of complex **2** recorded at different time interval in 0.1 M neutral phosphate buffer. (b) UV-visible spectra of 0.05 mM solution of complex **2** recorded at different time interval in 0.1 M neutral phosphate buffer.

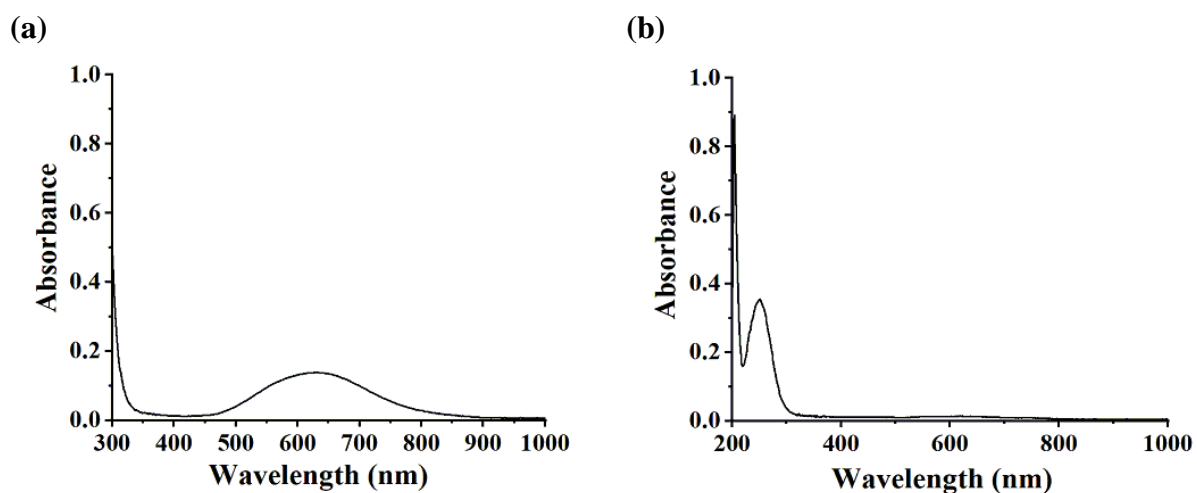


**Fig. S18** UV-visible spectra of (a) 1 mM solution and (b) 0.05 mM solution of complex **3** in 0.1 M neutral phosphate buffer.

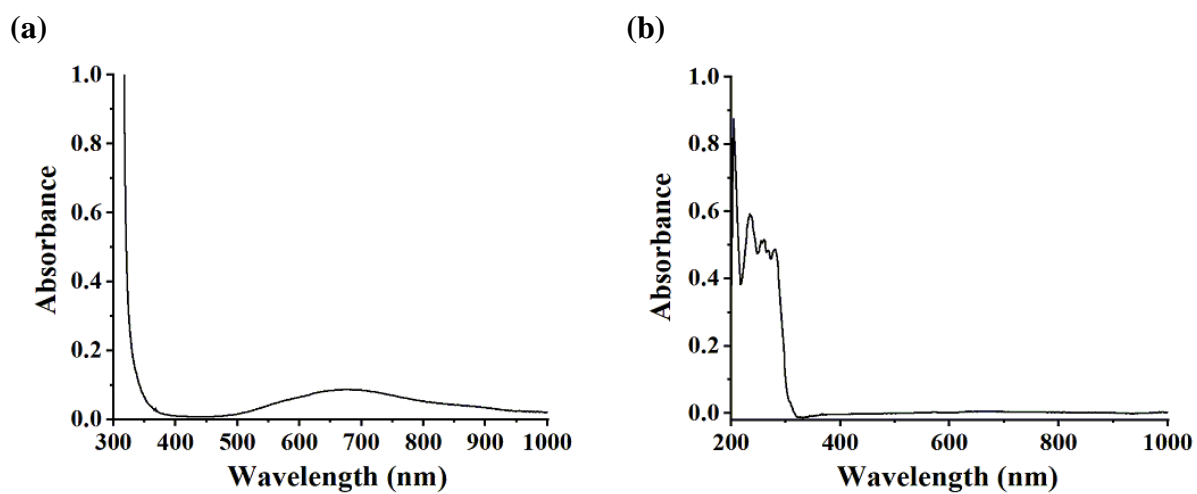


**Fig. S19** UV-visible spectra of (a) 1 mM solution and (b) 0.05 mM solution of complex **4** in 0.1 M neutral phosphate buffer.

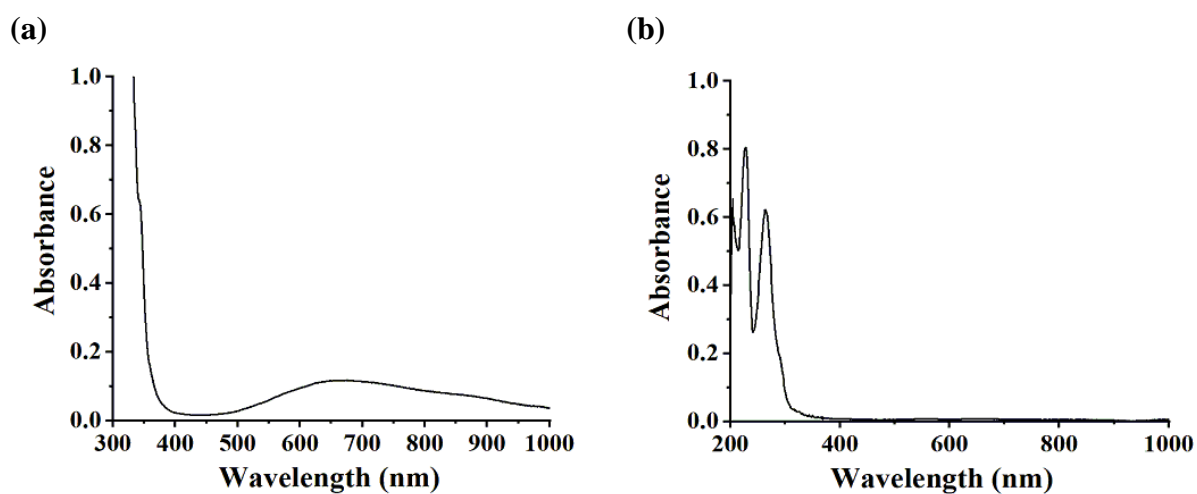


**Fig. S20** UV-visible spectra of (a) 1 mM solution and (b) 0.05 mM solution of complex **5** in 0.1 M neutral phosphate buffer.

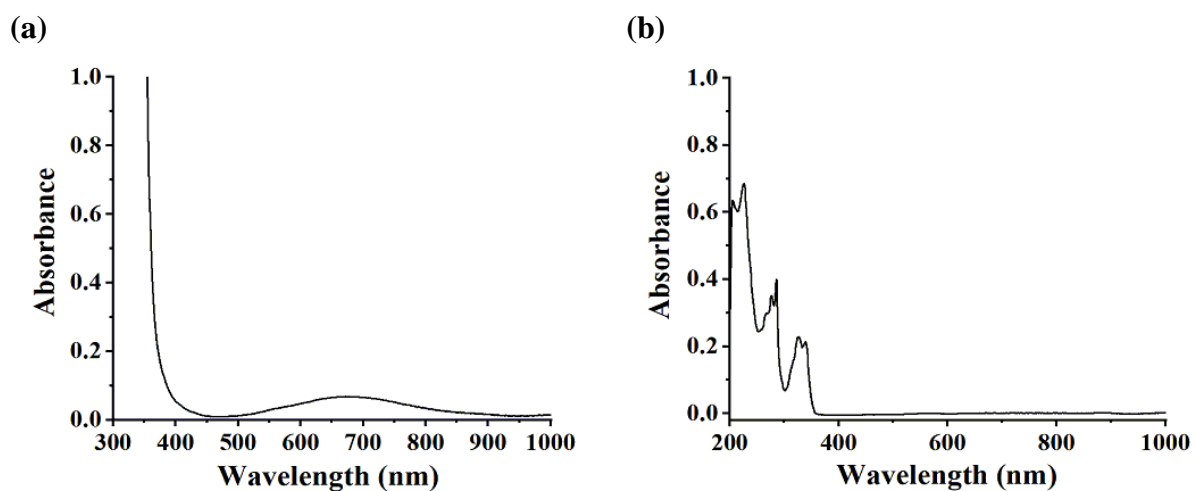


**Fig. S21** UV-visible spectra of (a) 1 mM solution and (b) 0.05 mM solution of complex 6 in 0.1 M neutral phosphate buffer.

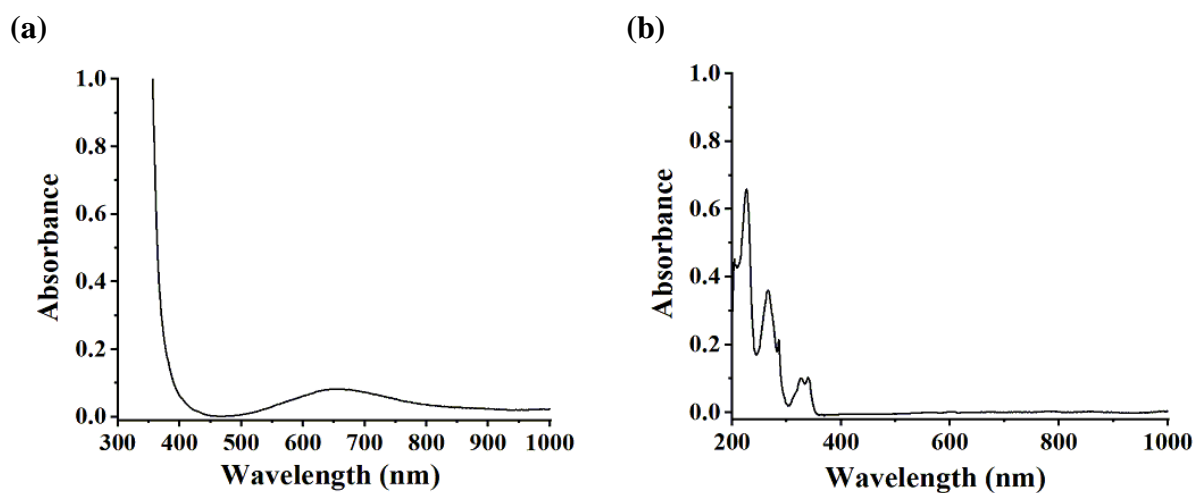


**Fig. S22** UV-visible spectra of (a) 1 mM solution and (b) 0.05 mM solution of complex 7 in 0.1 M neutral phosphate buffer.

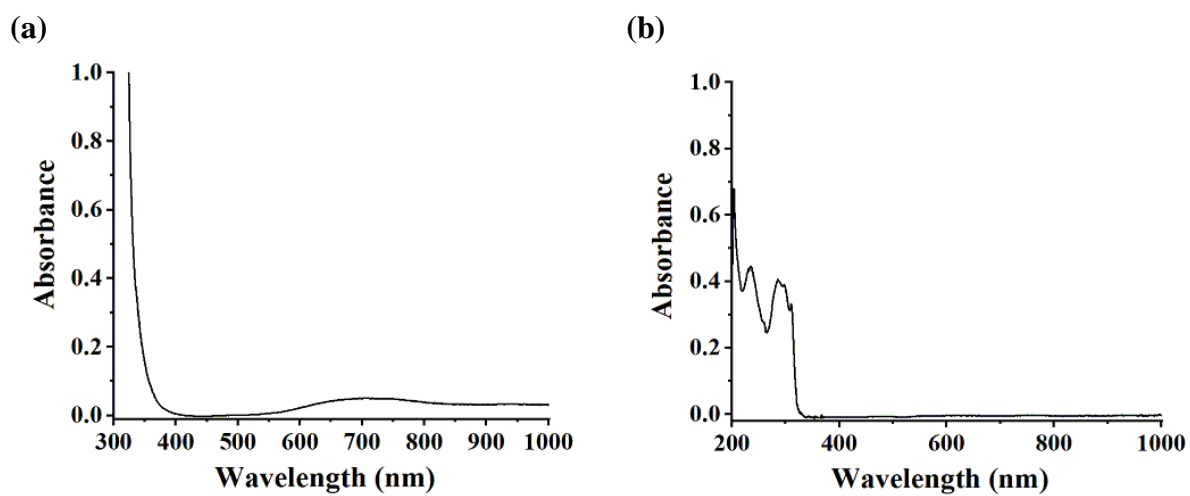


**Fig. S23** UV-visible spectra of (a) 1 mM solution and (b) 0.05 mM solution of complex  $[\text{Cu}(\text{bipy})_2](\text{ClO}_4)_2$  in 0.1 M neutral phosphate buffer.

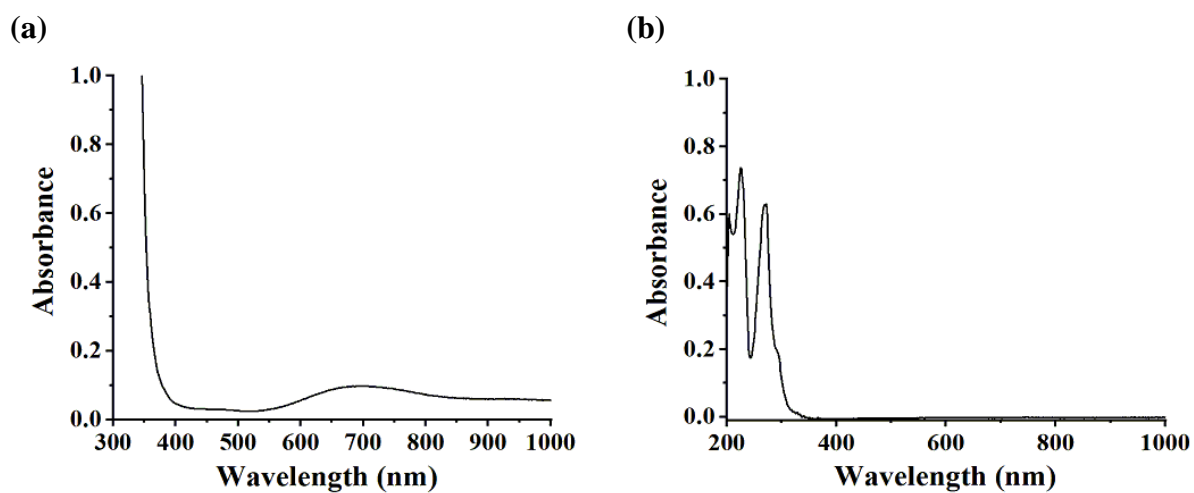


**Fig. S24** UV-visible spectra of (a) 1 mM solution and (b) 0.05 mM solution of complex  $[\text{Cu}(\text{phen})_2](\text{ClO}_4)_2$  in 0.1 M neutral phosphate buffer.

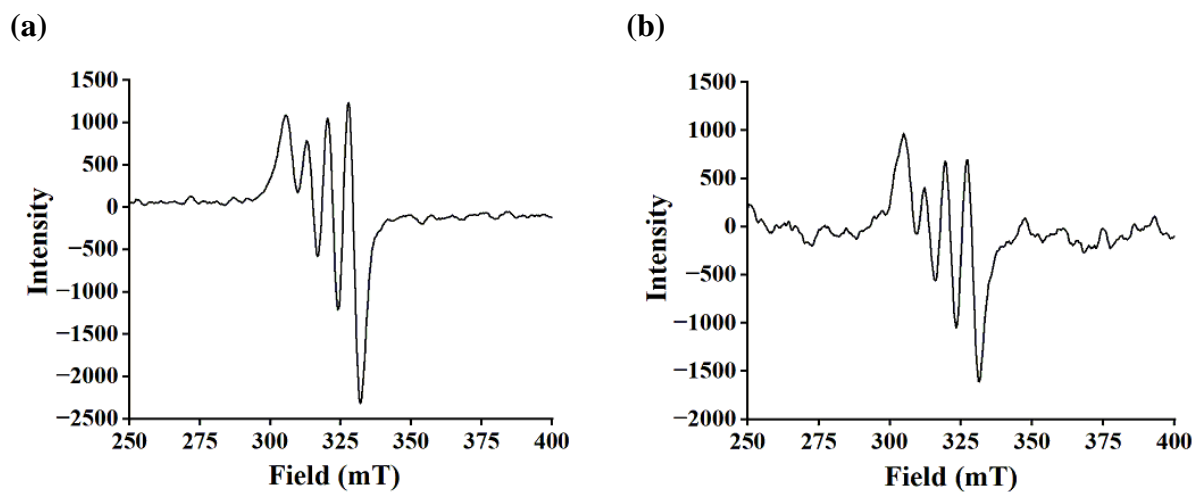


**Fig. S25** EPR spectra of (a) Complex 1 and (b) Complex 2 in 0.1 M neutral phosphate buffer.

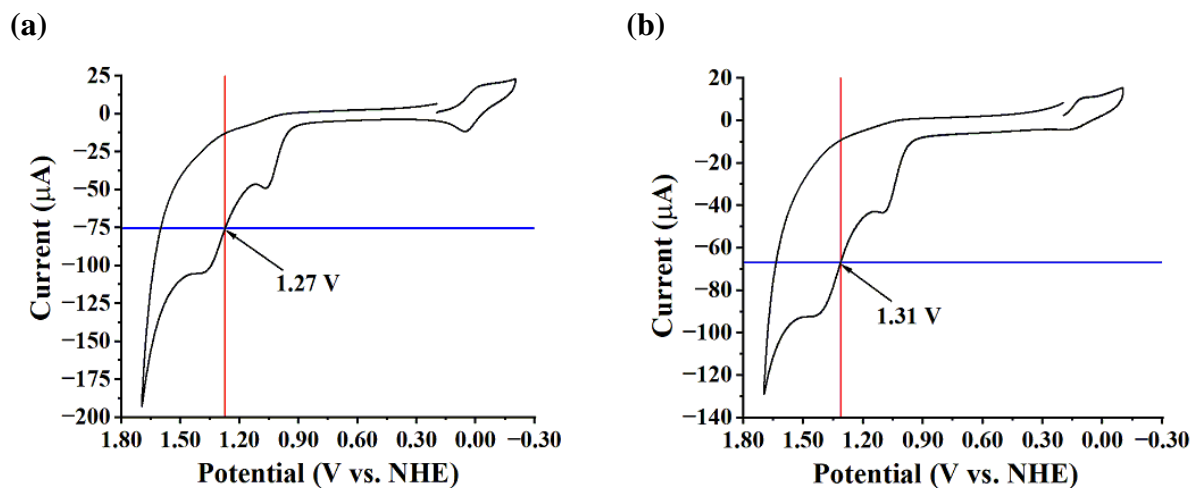


**Fig. S26** Cyclic voltammogram of 1 mM solution of (a) complex 1 and (b) complex 2 in 0.1 M neutral phosphate at  $100 \text{ mVs}^{-1}$  scan rate. The onset potentials for water oxidation located near 1.27 V and 1.31 V vs. NHE for complexes 1 and 2, respectively.

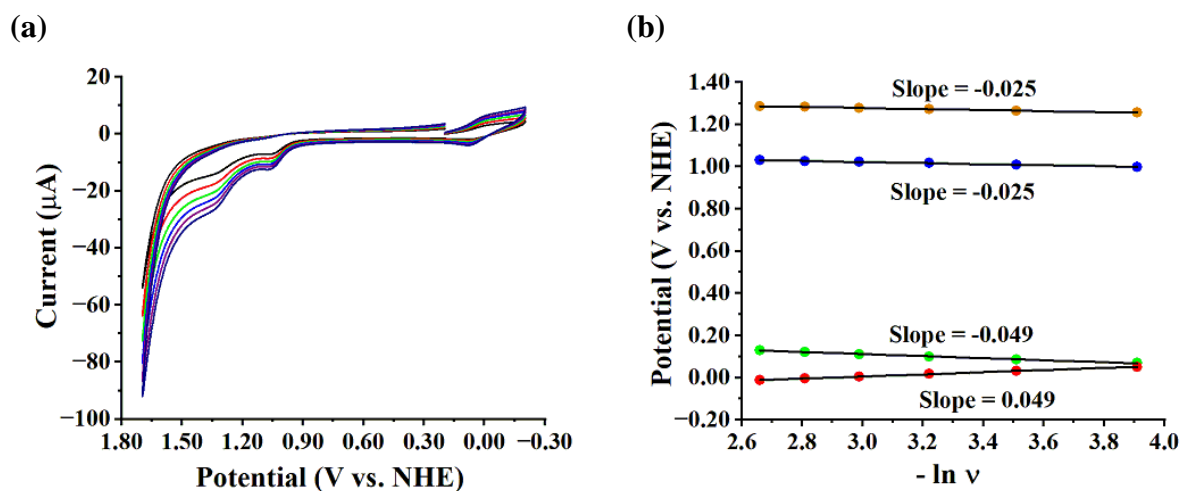


**Fig. S27** (a) Cyclic voltammograms of complex **1** at 20 (black), 30 (red), 40 (green), 50 (blue), 60 (purple) and 70 (navy) mVs<sup>-1</sup> scan rates in 0.1 M neutral phosphate buffer. (b) Plot of  $-\ln v$  vs. potential of complex **1** for cathodic current of Cu(II)-Cu(I) couple (red dot), anodic current of Cu(II)-Cu(I) couple (green dot), 2<sup>nd</sup> anodic peak (blue dot) and 3<sup>rd</sup> anodic peak (orange dot).

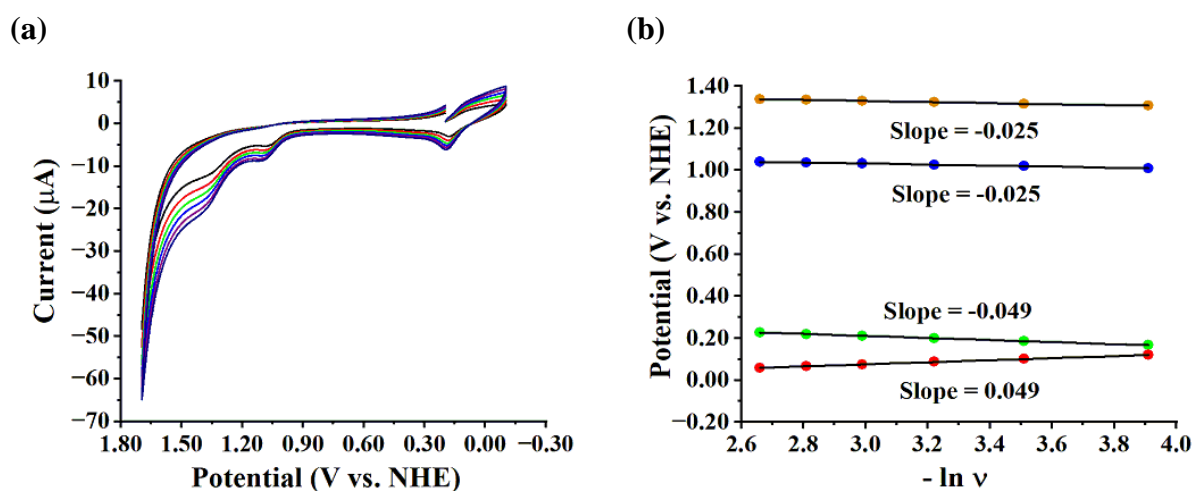


**Fig. S28** (a) Cyclic voltammograms of complex **2** at 20 (black), 30 (red), 40 (green), 50 (blue), 60 (purple) and 70 (navy) mVs<sup>-1</sup> scan rates in 0.1 M neutral phosphate buffer. (b) Plot of  $-\ln v$  vs. potential of complex **2** for cathodic current of Cu(II)-Cu(I) couple (red dot), anodic current of Cu(II)-Cu(I) couple (green dot), 2<sup>nd</sup> anodic peak (blue dot) and 3<sup>rd</sup> anodic peak (orange dot).

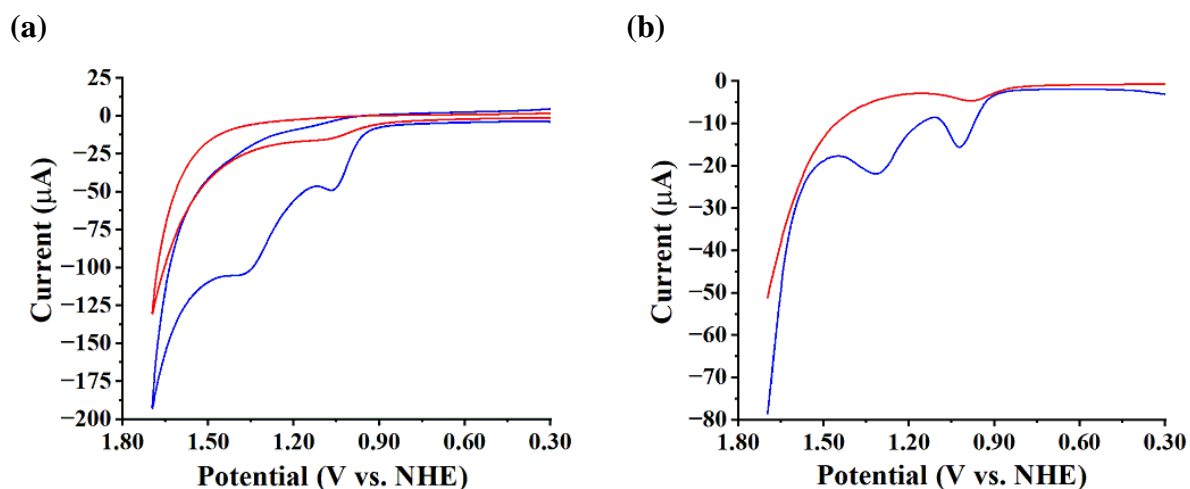


**Fig. S29** (a) Cyclic voltammograms and (b) Differential Pulse voltammograms of complex **1** (blue), and analogous Zn complex,  $[\text{Zn}(\text{bipy})(\text{HL}_1)](\text{ClO}_4)_2$  (red) in 0.1 M neutral phosphate buffer recorded with a glassy carbon (GC) working electrode, a Ag/AgCl reference electrode and a Pt counter electrode, scan rate  $100 \text{ mVs}^{-1}$ .

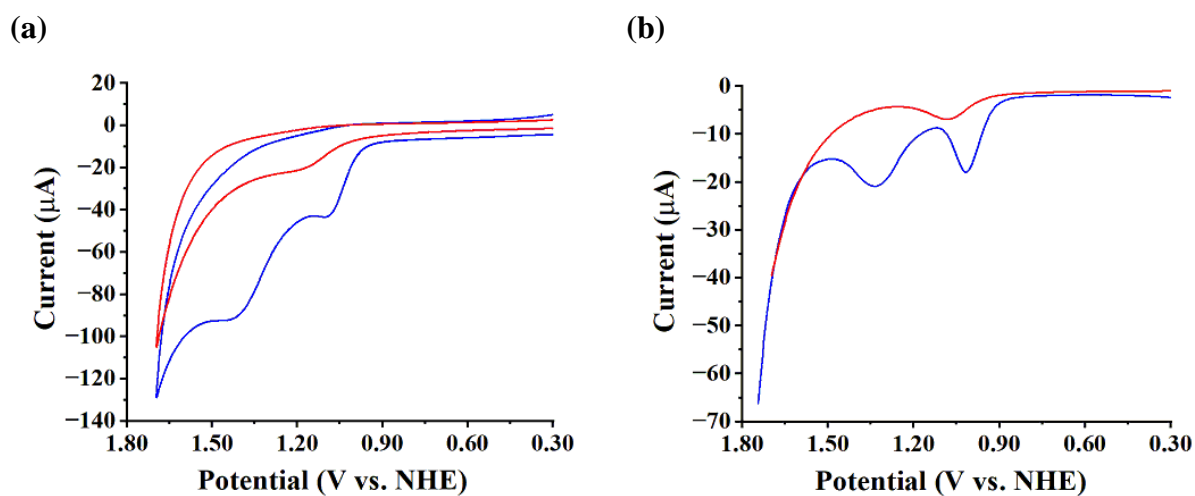


**Fig. S30** (a) Cyclic voltammograms and (b) Differential Pulse voltammograms of complex **2** (blue), and analogous Zn complex,  $[\text{Zn}(\text{phen})(\text{HL}_1)](\text{ClO}_4)_2$  (red) in 0.1 M neutral phosphate buffer recorded with a glassy carbon (GC) working electrode, a Ag/AgCl reference electrode and a Pt counter electrode, scan rate  $100 \text{ mVs}^{-1}$ .

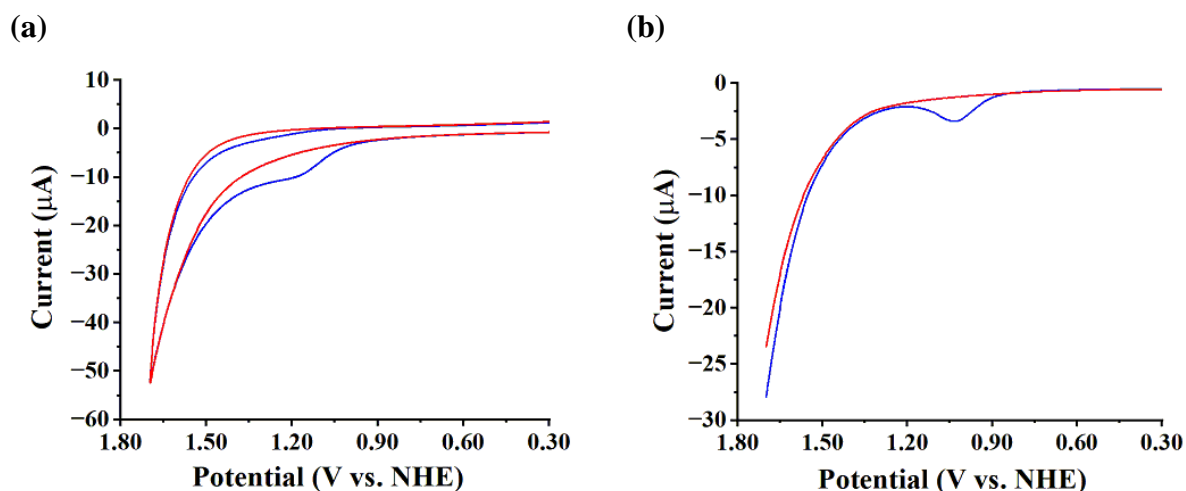


**Fig. S31** (a) Cyclic voltammograms and (b) Differential Pulse voltammograms of ligand **HL<sub>1</sub>**, **N<sup>1</sup>-(2-aminoethyl)ethane-1,2-diamine** (blue), and its **N<sup>1</sup>-methylated form**, **N<sup>1</sup>-(2-aminoethyl)-N<sup>1</sup>-methylethane-1,2-diamine** (red) in 0.1 M neutral phosphate buffer recorded with a glassy carbon (GC) working electrode, a Ag/AgCl reference electrode and a Pt counter electrode, scan rate 100 mVs<sup>-1</sup>.

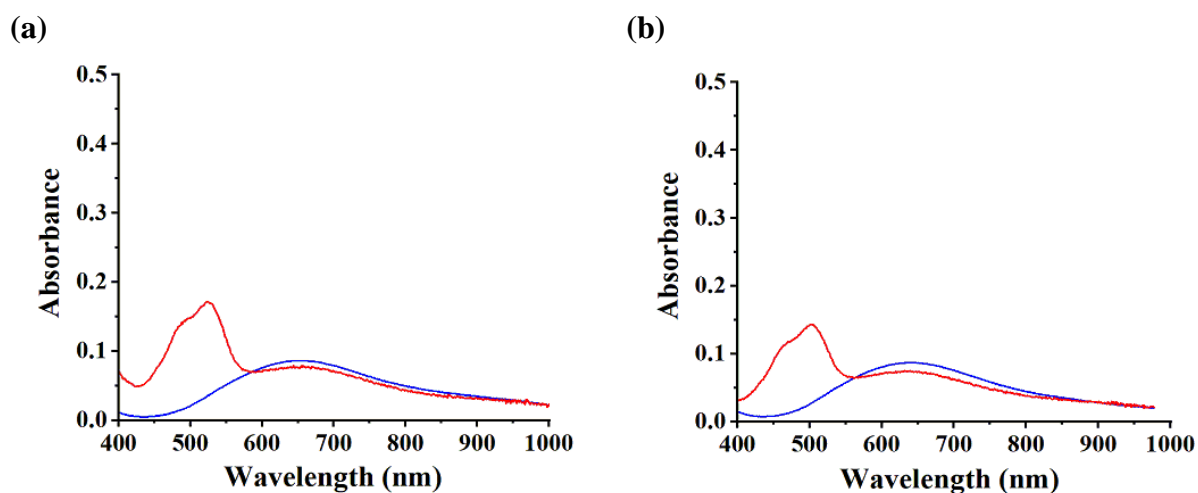


**Fig. S32** UV-visible spectra of (a) complex **1** and (b) complex **2** before electrolysis (blue), and during electrolysis (red) at 1.02 V and 1.01 V vs. NHE respectively in 0.1 M neutral phosphate buffer.

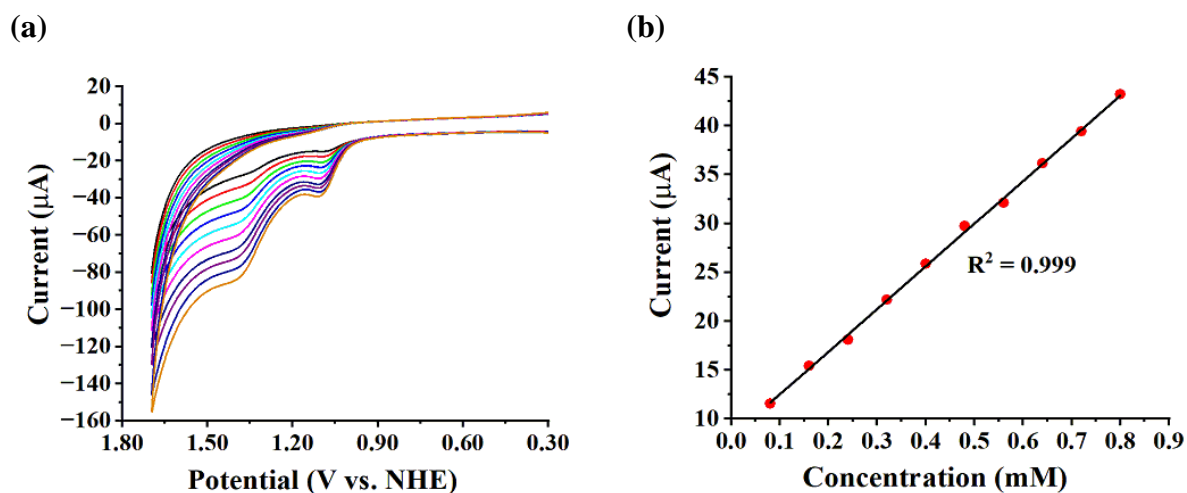


**Fig. S33** (a) Cyclic voltammograms of complex **1** at 0.08 (black), 0.16 (red), 0.24 (green), 0.32 (blue), 0.40 (cyan), 0.48 (magenta), 0.56 (navy), 0.64 (purple), 0.72 (royal), 0.80 (orange) and 0.88 mM (violet) concentration in 0.1 M neutral phosphate buffer. Scan rate:  $100 \text{ mVs}^{-1}$ . (b) Catalytic current at 1.32 V vs. NHE for complex **1** as a function of the catalyst concentration from 0.08 mM to 0.88 mM in 0.1 M neutral phosphate buffer.

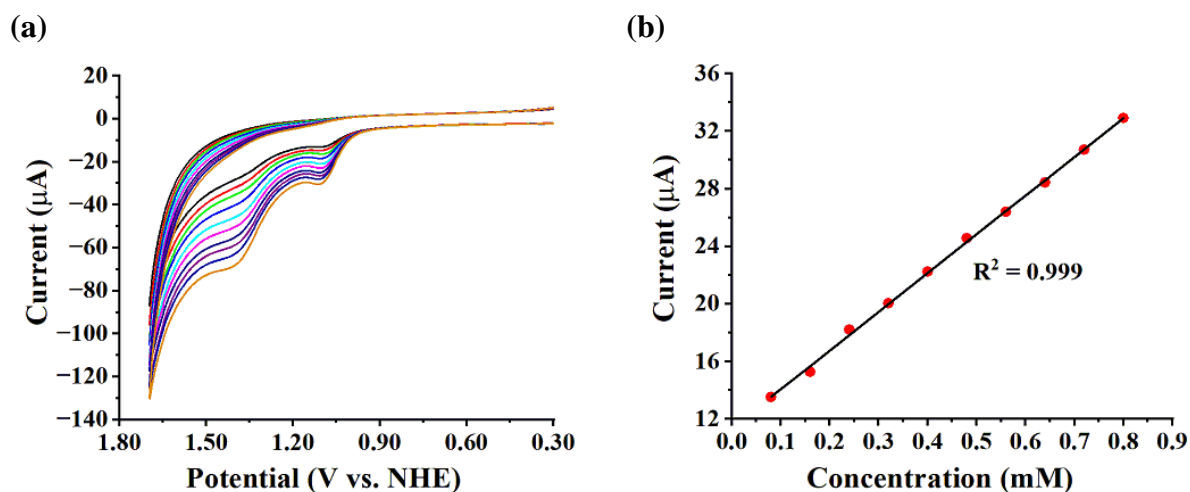


**Fig. S34** (a) Cyclic voltammograms of complex **2** at 0.08 (black), 0.16 (red), 0.24 (green), 0.32 (blue), 0.40 (cyan), 0.48 (magenta), 0.56 (navy), 0.64 (purple), 0.72 (royal), 0.80 (orange) and 0.88 mM (violet) concentration in 0.1 M neutral phosphate buffer. Scan rate:  $100 \text{ mVs}^{-1}$ . (b) Catalytic current at 1.34 V vs. NHE for complex **2** as a function of the catalyst concentration from 0.08 mM to 0.88 mM in 0.1 M neutral phosphate buffer.

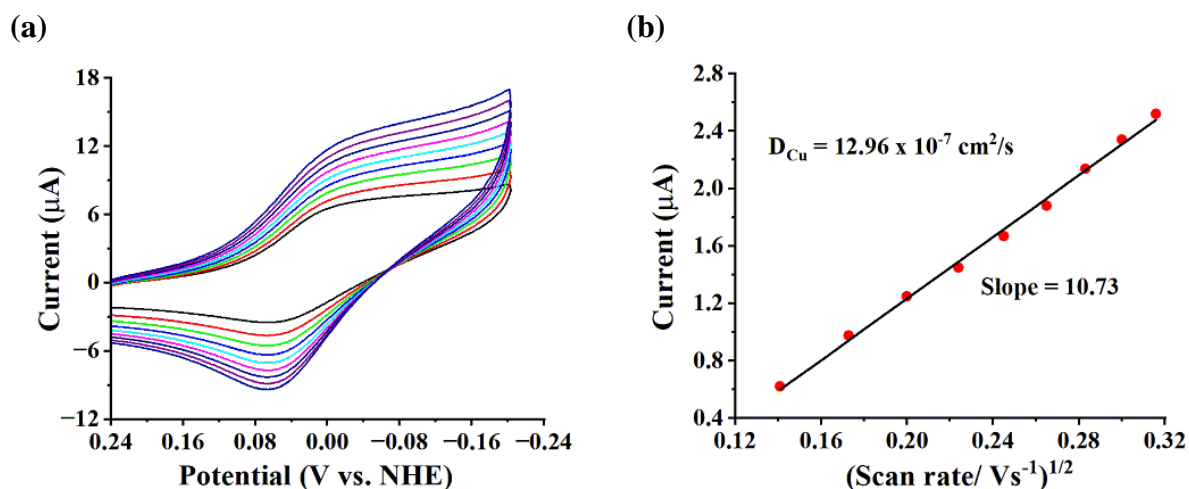


**Fig. S35** (a) Cyclic voltammograms of complex **1** in the range 0.24 to -0.24 V vs. NHE at 20 (black), 30 (red), 40 (green), 50 (blue), 60 (cyan), 70 (magenta), 80 (navy), 90 (purple) and 100 (royal) mVs<sup>-1</sup> scan rate. (b) Dependence of the peak current for the Cu<sup>II</sup>/Cu<sup>I</sup> couple of complex **1** on the square root of scan rate with standard three electrode system in 0.1 M neutral phosphate buffer.  $D_{Cu} = 12.96 \times 10^{-7} \text{ cm}^2/\text{s}$ .

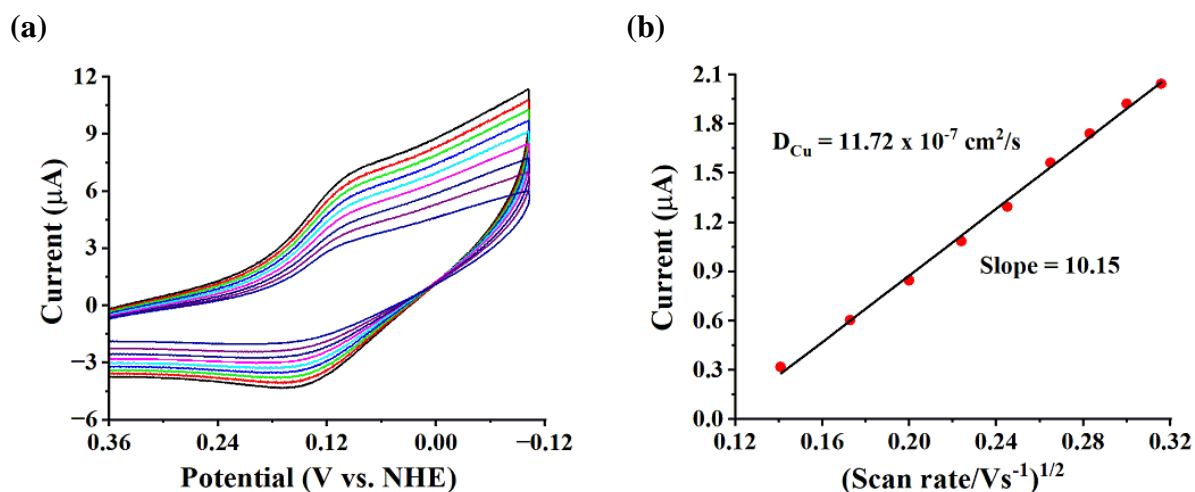


**Fig. S36** (a) Cyclic voltammograms of complex **2** in the range 0.36 to -0.12 V vs. NHE at 20 (black), 30 (red), 40 (green), 50 (blue), 60 (cyan), 70 (magenta), 80 (navy), 90 (purple) and 100 (royal) mVs<sup>-1</sup> scan rate. (b) Dependence of the peak current for the Cu<sup>II</sup>/Cu<sup>I</sup> couple of complex **2** on the square root of scan rate with standard three electrode system in 0.1 M neutral phosphate buffer.  $D_{Cu} = 11.72 \times 10^{-7} \text{ cm}^2/\text{s}$ .

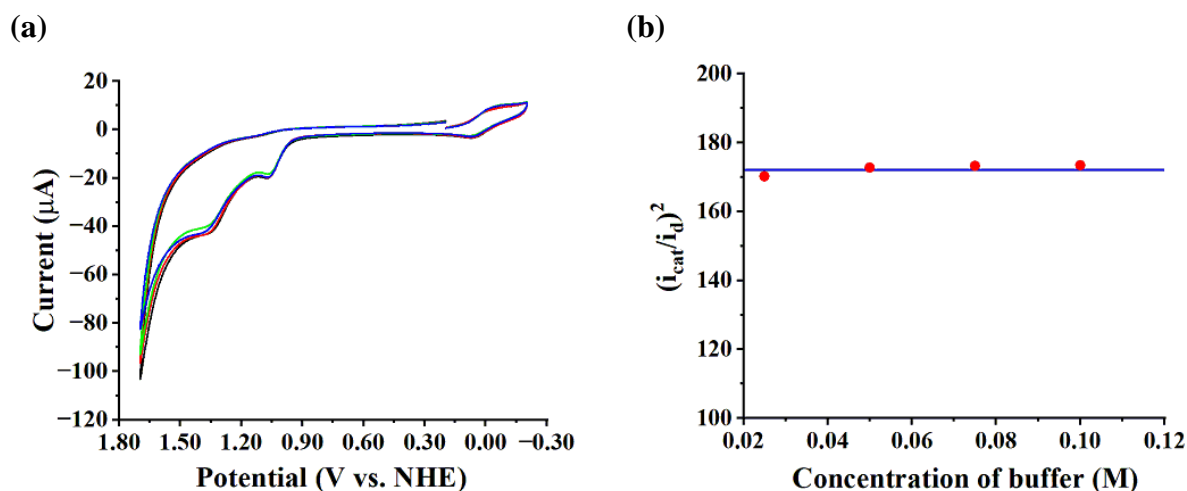


**Fig. S37** (a) Cyclic voltammograms of 0.5 mM solution of complex **1** in 0.1 M (black), 0.075 M (red), 0.05 M (blue) and 0.025 M (green) neutral phosphate buffer at a scan rate of  $100 \text{ mVs}^{-1}$ . (b) Plot of  $(i_{\text{cat}}/i_{\text{d}})^2$  vs. different concentration of buffer for 0.5 mM solution of complex **1**.

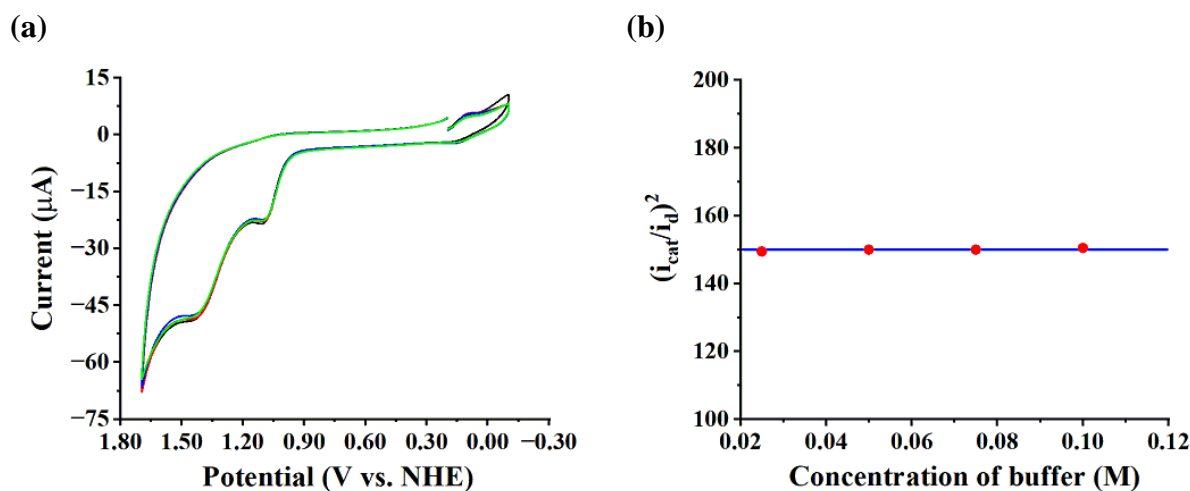


**Fig. S38** (a) Cyclic voltammograms of 0.5 mM solution of complex **2** in 0.1 M (black), 0.075 M (red), 0.05 M (blue) and 0.025 M (green) neutral phosphate buffer at a scan rate of  $100 \text{ mVs}^{-1}$ . (b) Plot of  $(i_{\text{cat}}/i_{\text{d}})^2$  vs. different concentration of buffer for 0.5 mM solution of complex **2**.

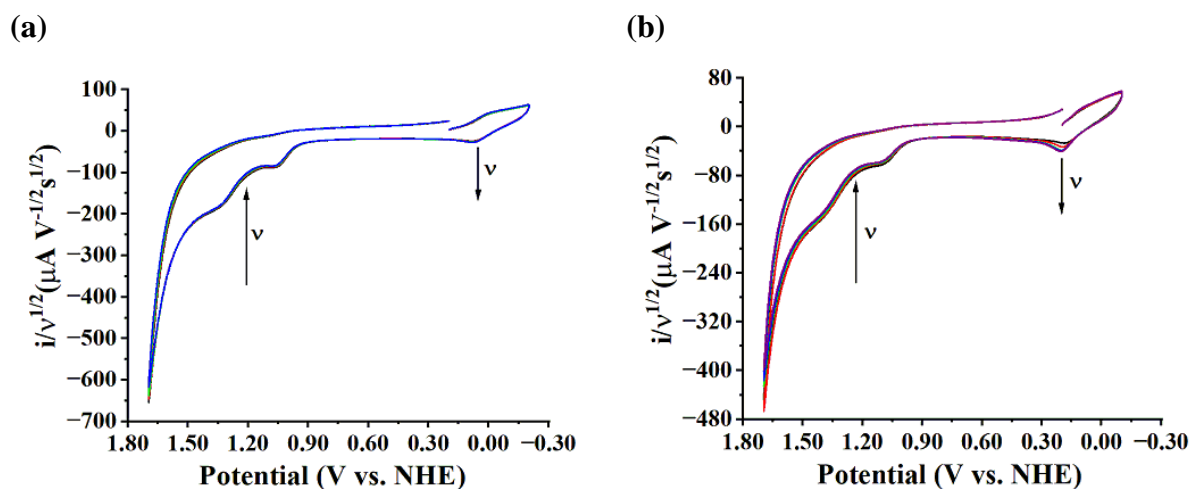


**Fig. S39** (a) Cyclic voltammograms of complex **1** with currents normalized to the square root of the scan rates 30 (black), 40 (red), 50 (green) and 70 ( $\text{mVs}^{-1}$ ) measured in 0.1 M neutral phosphate buffer. (b) Cyclic voltammograms of complex **2** with currents normalized to the square root of the scan rates 20 (black), 30 (red), 60 (green), 70 (blue) and 90 ( $\text{mVs}^{-1}$ ) measured in 0.1 M neutral phosphate buffer

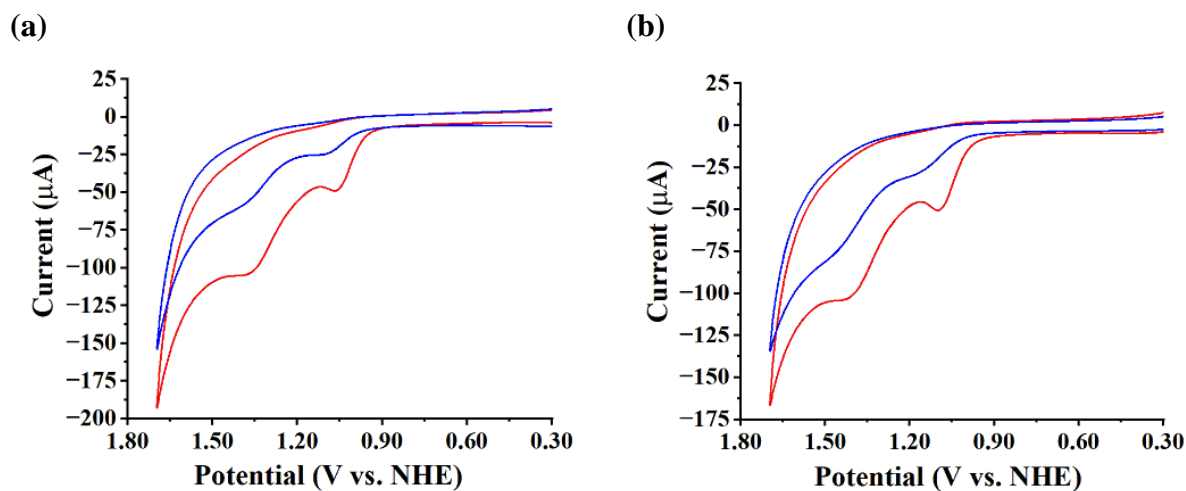


**Fig. S40** Cyclic voltammograms of (a) complex **1** and (b) complex **2** in  $\text{H}_2\text{O}$  (Red) and  $\text{D}_2\text{O}$  (Black) 0.1 M phosphate buffer recorded with a glassy carbon (GC) working electrode, a Ag/AgCl reference electrode and a Pt counter electrode. Scan rate,  $100 \text{ mVs}^{-1}$ .

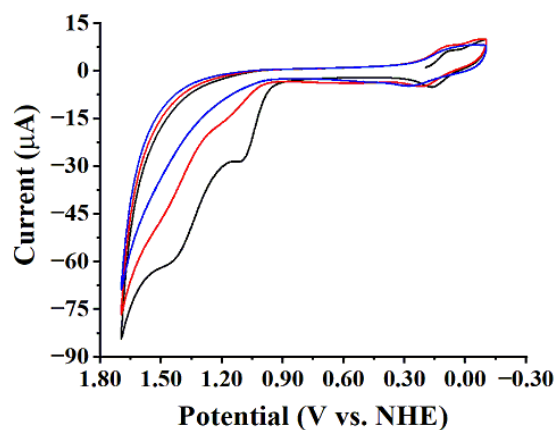


**Fig. S41** Cyclic voltammograms (7 sweeps) of complex **3** recorded in 0.1 M neutral phosphate buffer at scan rate  $100 \text{ mVs}^{-1}$ . Black line corresponds to sweeps 1-3, red line for sweeps 4-5 and blue line for sweeps 6-7.

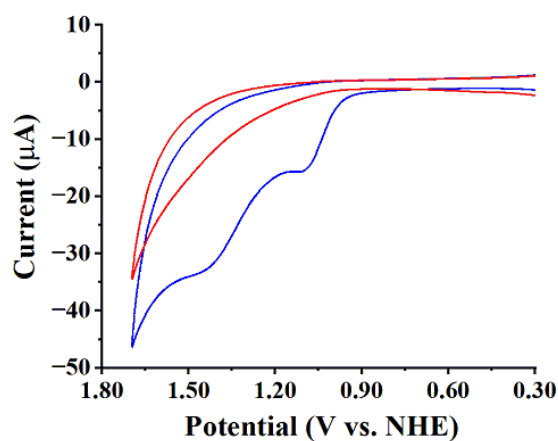


**Fig. S42** Cyclic voltammograms of complex **3** recorded before (blue) and after (red) bulk electrolysis at 1.35 V vs. NHE in 0.1 M neutral phosphate buffer using glassy carbon (GC) as working electrode (area  $0.07 \text{ cm}^2$ ), Ag/AgCl as reference electrode and Pt as counter electrode. Scan rate,  $100 \text{ mVs}^{-1}$ .

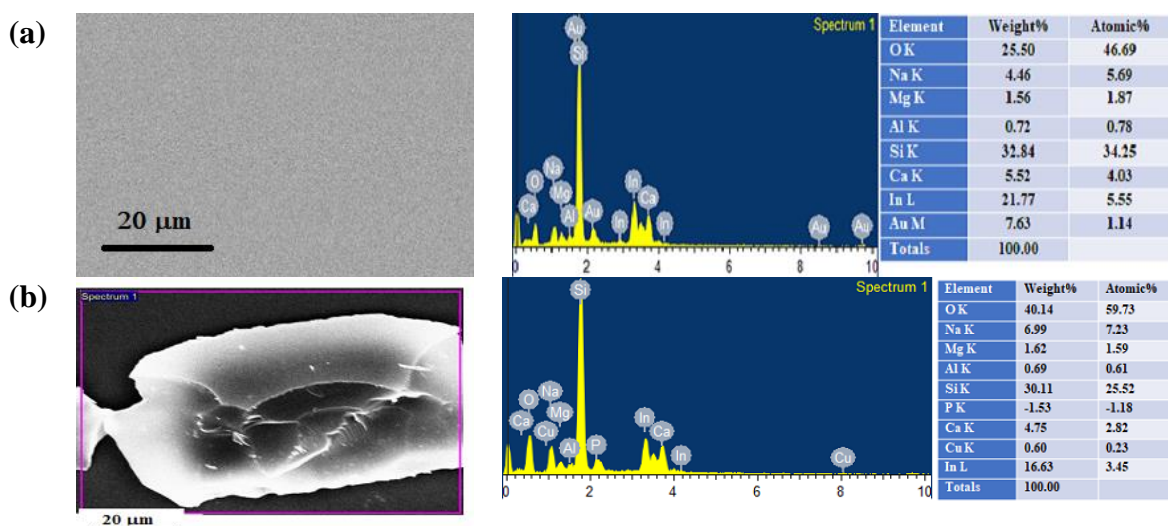


**Fig. S43** FE-SEM and EDX plot of (a) fresh ITO working electrode (b) ITO working electrode after bulk electrolysis of complex **3** in 0.1 M neutral phosphate buffer.

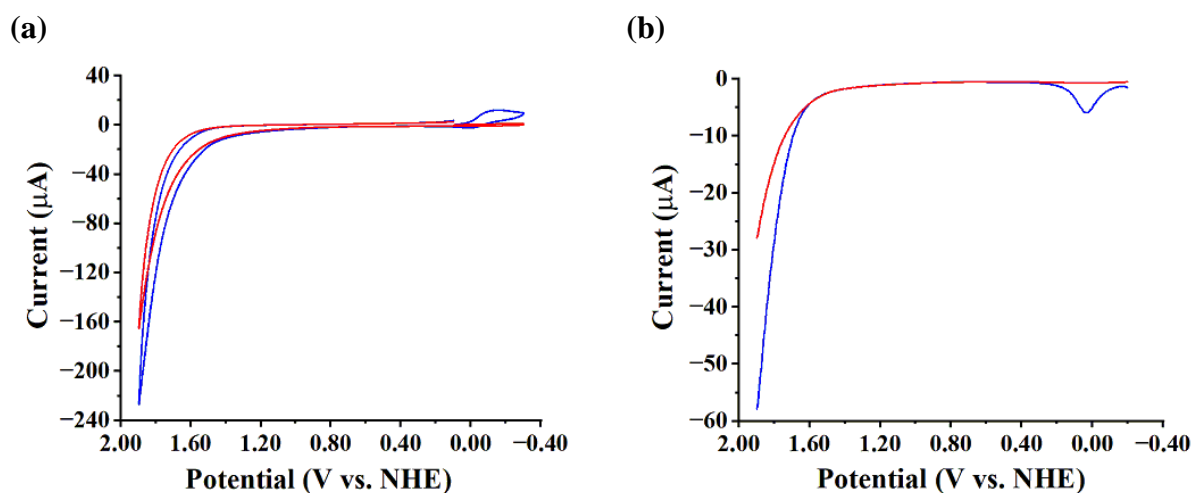


**Fig. S44** (a) Cyclic voltammogram of 1 mM solution of complex  $[\text{Cu}(\text{bipy})_2](\text{ClO}_4)_2$  (blue line) in 0.1 M neutral phosphate buffer at a scan rate of  $100 \text{ mVs}^{-1}$ . The red line indicates the cyclic voltammogram of 0.1 M neutral phosphate buffer in absence of complex at a scan rate of  $100 \text{ mVs}^{-1}$ . (b) Differential pulse voltammogram of 1 mM solution of complex  $[\text{Cu}(\text{bipy})_2](\text{ClO}_4)_2$  (blue line) in 0.1 M neutral phosphate buffer. The red line indicates the differential pulse voltammogram of 0.1 M neutral phosphate buffer in absence of complex.

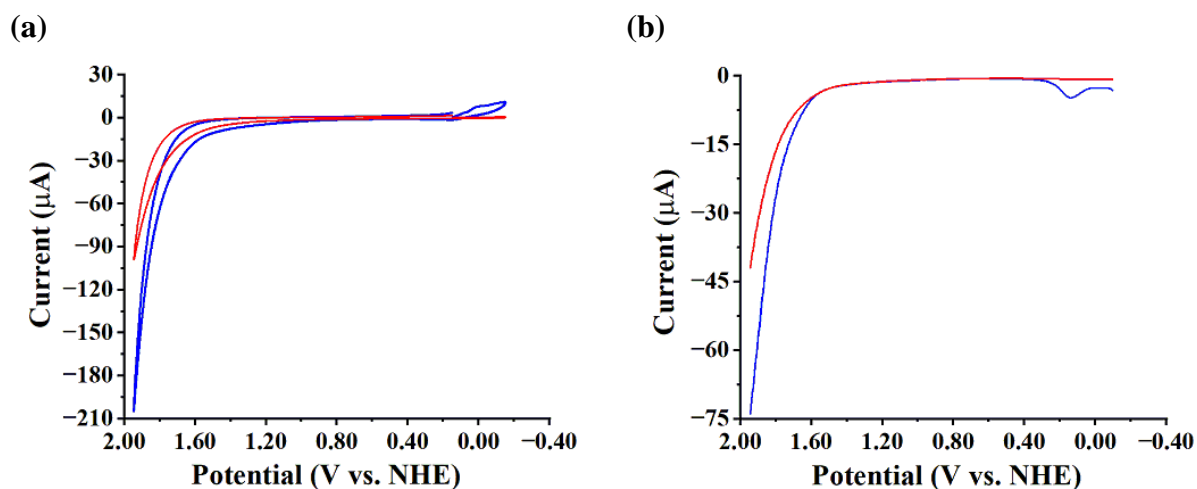


**Fig. S45** (a) Cyclic voltammogram of 1 mM solution of complex  $[\text{Cu}(\text{phen})_2](\text{ClO}_4)_2$  (blue line) in 0.1 M neutral phosphate buffer at a scan rate of  $100 \text{ mVs}^{-1}$ . The red line indicates the cyclic voltammogram of 0.1 M neutral phosphate buffer in absence of complex at a scan rate of  $100 \text{ mVs}^{-1}$ . (b) Differential pulse voltammogram of 1 mM solution of complex  $[\text{Cu}(\text{phen})_2](\text{ClO}_4)_2$  (blue line) in 0.1 M neutral phosphate buffer at. The red line indicates the differential pulse voltammogram of 0.1 M neutral phosphate buffer in absence of complex.

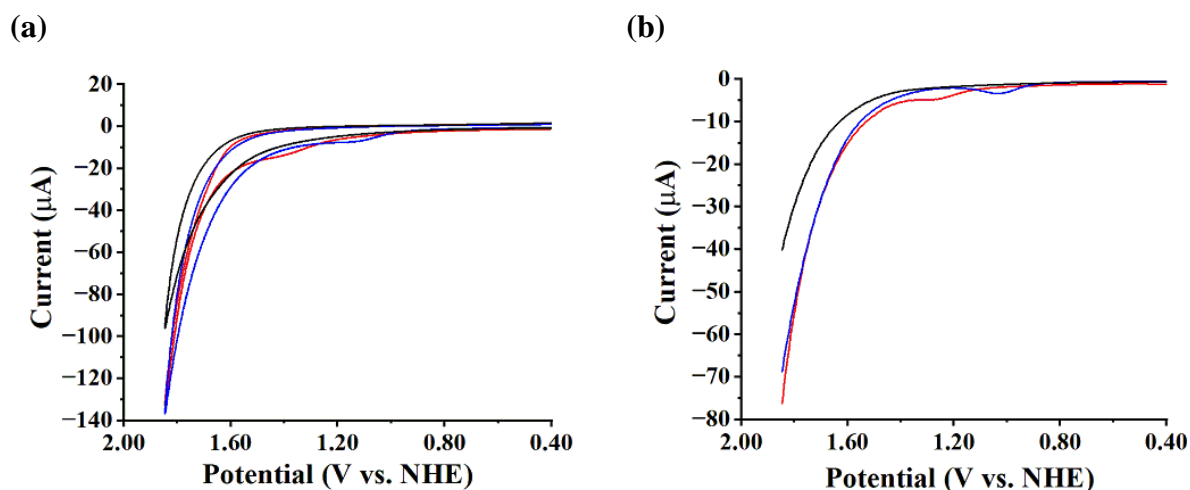


**Fig. S46** (a) Cyclic voltammograms and (b) Differential Pulse voltammograms of ligands **HL<sub>1</sub>**, **N<sup>1</sup>-(2-aminoethyl)ethane-1,2-diamine** (blue), **HL<sub>2</sub>**, **bis(pyridin-2-ylmethyl)amine** (red) and **L<sub>3</sub>**, **2,6-di(pyridin-2-yl)pyridine** (black) in 0.1 M neutral phosphate buffer recorded with a glassy carbon (GC) working electrode, a Ag/AgCl reference electrode and a Pt counter electrode, scan rate  $100 \text{ mVs}^{-1}$ .

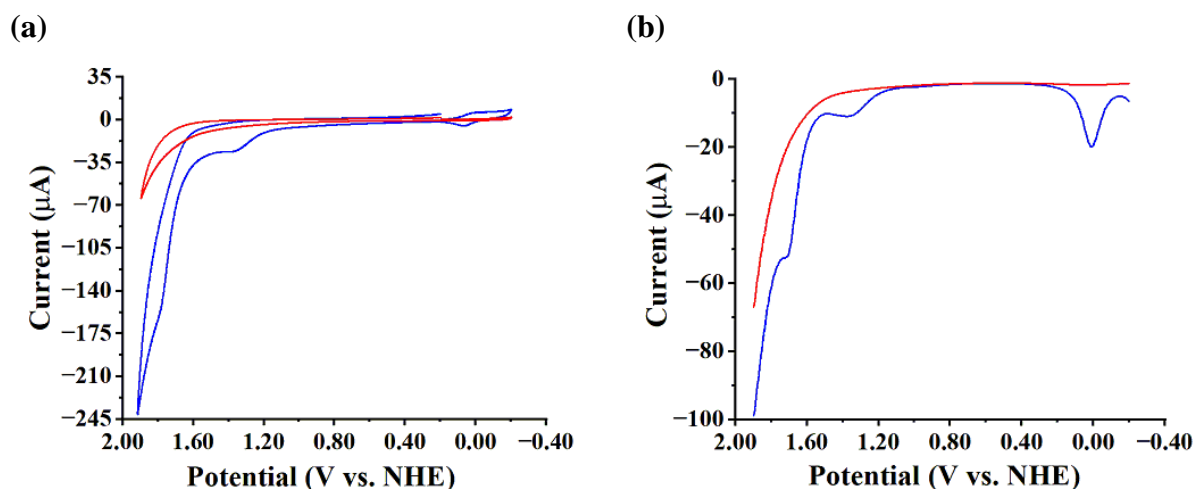


**Fig. S47** (a) Cyclic voltammogram of 1 mM solution of complex **4** (blue line) in 0.1 M neutral phosphate buffer at a scan rate of  $100 \text{ mVs}^{-1}$ . The red line indicates the cyclic voltammogram of 0.1 M neutral phosphate buffer in absence of complex at a scan rate of  $100 \text{ mVs}^{-1}$ . (b) Differential pulse voltammogram of 1 mM solution of complex **4** (blue line) in 0.1 M neutral phosphate buffer. The red line indicates the differential pulse voltammogram of 0.1 M neutral phosphate buffer in absence of complex.

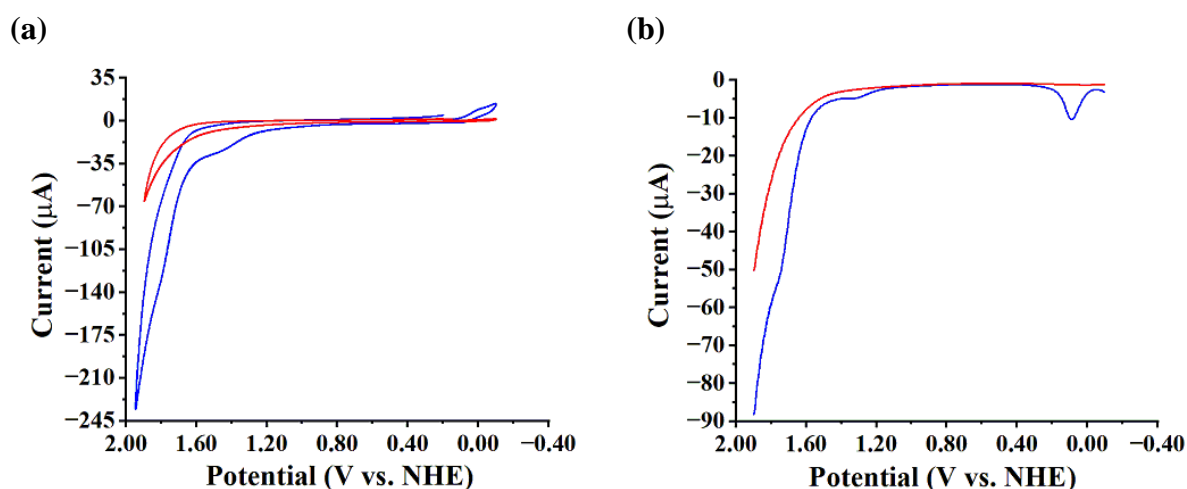


**Fig. S48** (a) Cyclic voltammogram of 1 mM solution of complex **5** (blue line) in 0.1 M neutral phosphate buffer at a scan rate of  $100 \text{ mVs}^{-1}$ . The red line indicates the cyclic voltammogram of 0.1 M neutral phosphate buffer in absence of complex at a scan rate of  $100 \text{ mVs}^{-1}$ . (b) Differential pulse voltammogram of 1 mM solution of complex **5** (blue line) in 0.1 M neutral phosphate buffer. The red line indicates the differential pulse voltammogram of 0.1 M neutral phosphate buffer in absence of complex.

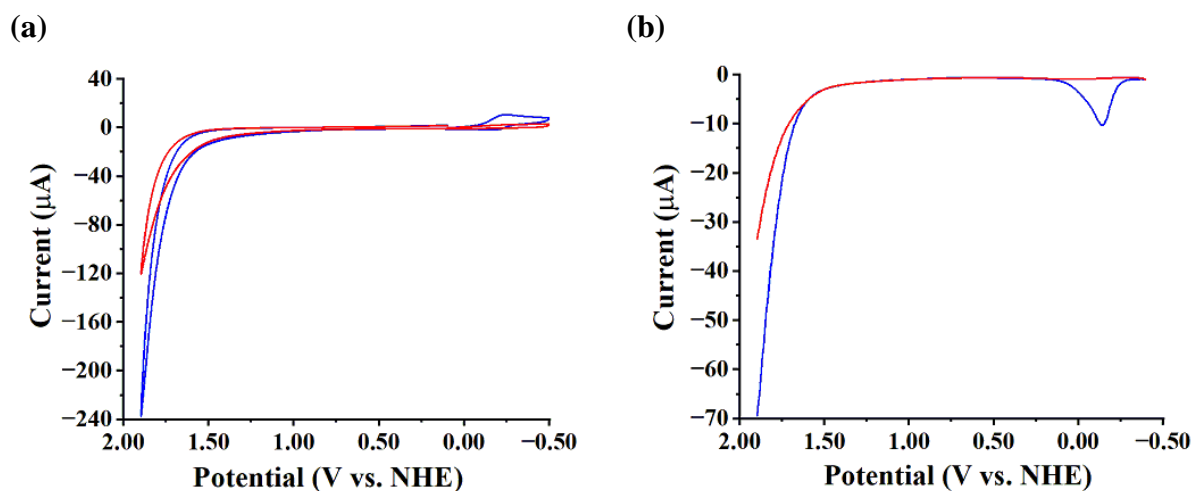


**Fig. S49** (a) Cyclic voltammogram of 1 mM solution of complex **6** (blue line) in 0.1 M neutral phosphate buffer at a scan rate of  $100 \text{ mVs}^{-1}$ . The red line indicates the cyclic voltammogram of 0.1 M neutral phosphate buffer in absence of complex at a scan rate of  $100 \text{ mVs}^{-1}$ . (b) Differential pulse voltammogram of 1 mM solution of complex **6** (blue line) in 0.1 M neutral phosphate buffer. The red line indicates the differential pulse voltammogram of 0.1 M neutral phosphate buffer in absence of complex.

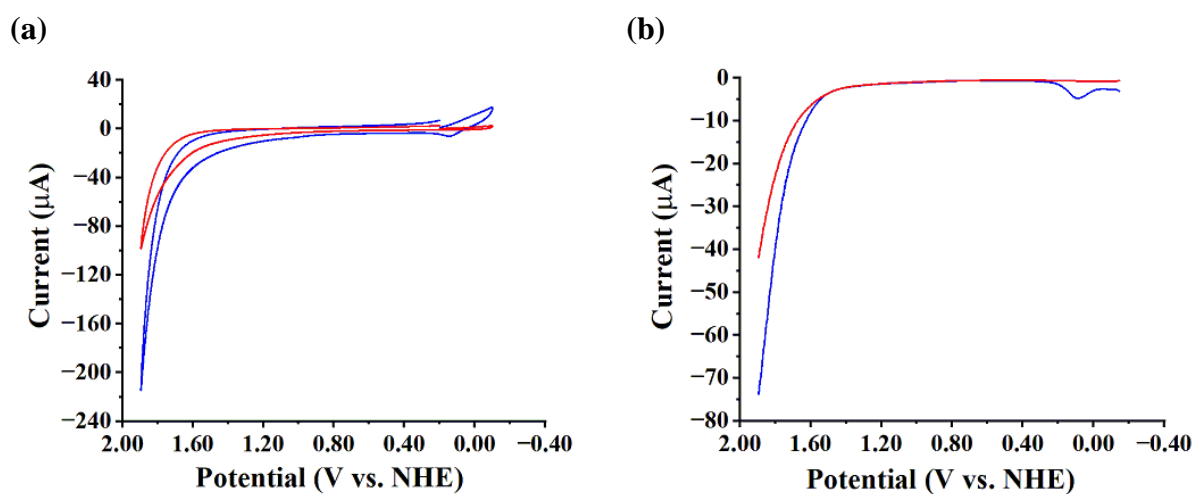


**Fig. S50** (a) Cyclic voltammogram of 1 mM solution of complex **7** (blue line) in 0.1 M neutral phosphate buffer at a scan rate of  $100 \text{ mVs}^{-1}$ . The red line indicates the cyclic voltammogram of 0.1 M neutral phosphate buffer in absence of complex at a scan rate of  $100 \text{ mVs}^{-1}$ . (b) Differential pulse voltammogram of 1 mM solution of complex **7** (blue line) in 0.1 M neutral phosphate buffer. The red line indicates the differential pulse voltammogram of 0.1 M neutral phosphate buffer in absence of complex.

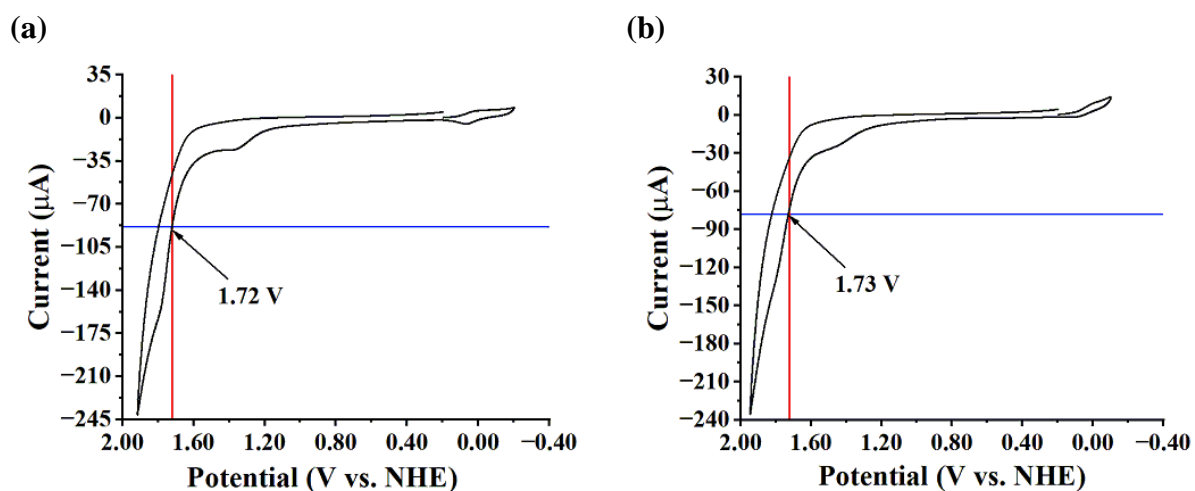


**Fig. S51** Cyclic voltammogram of 1 mM solution of (a) complex 4 and (b) complex 5 in 0.1 M neutral phosphate at  $100 \text{ mVs}^{-1}$  scan rate. The onset potentials for water oxidation located near 1.72 V and 1.73 V vs. NHE for complexes 4 and 5 respectively.

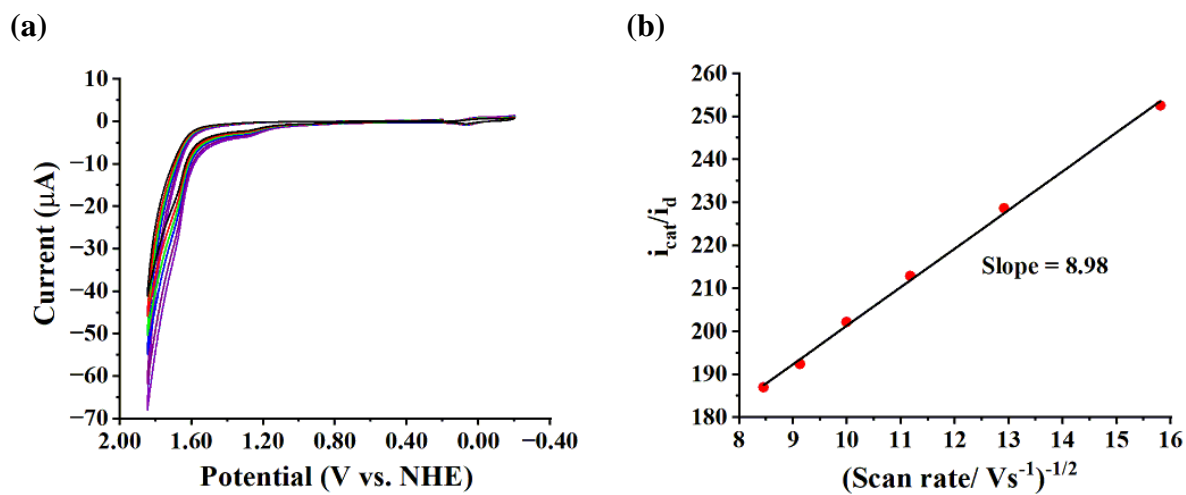


**Fig. S52** (a) Cyclic voltammograms of complex 4 at 4 (black), 6 (red), 8 (green), 10 (blue), 12 (purple) and 14 (violet)  $\text{mVs}^{-1}$  scan rates in 0.1 M neutral phosphate buffer. (b) Plot of  $i_{\text{cat}}/i_{\text{d}}$  vs.  $v^{-1/2}$  at each scan rate for complex 4.

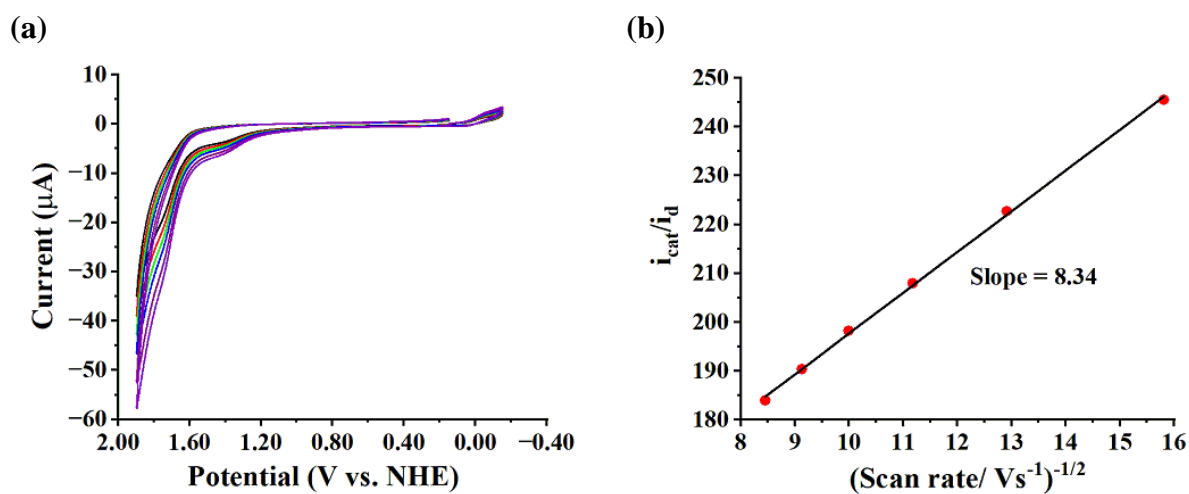


**Fig. S53** (a) Cyclic voltammograms of complex **5** at 4 (black), 6 (red), 8 (green), 10 (blue), 12 (purple) and 14 (violet) mVs<sup>-1</sup> scan rates in 0.1 M neutral phosphate buffer. (b) Plot of  $i_{cat}/i_d$  vs.  $v^{-1/2}$  at each scan rate for complex **5**.

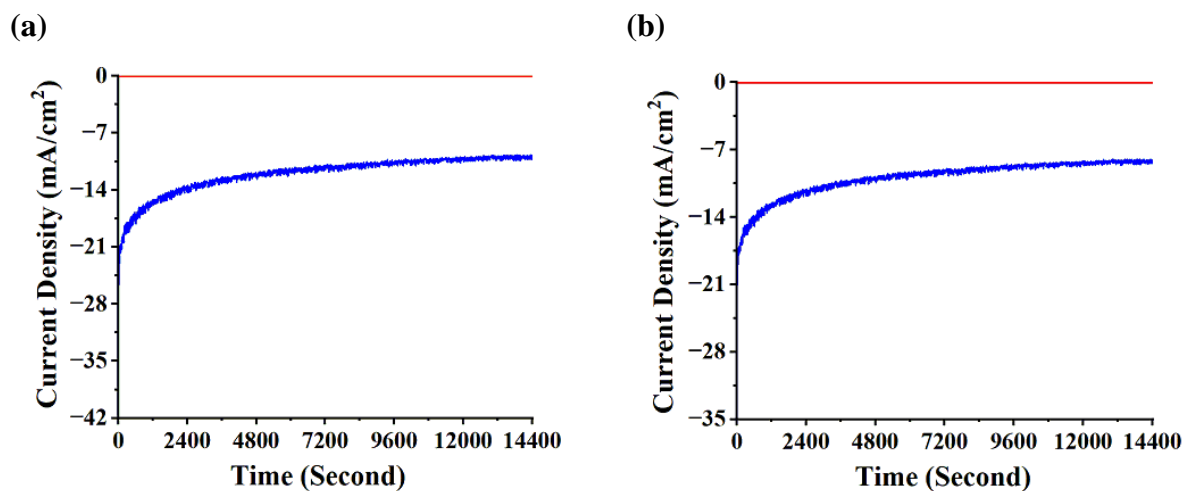


**Fig. S54** Plot of current density vs. time recorded during 4 hour of bulk electrolysis with (blue line) and without (red line) (a) complex **1** and (b) complex **2** in 0.1 M neutral phosphate buffer using ITO working electrode (area 4 cm<sup>2</sup>), Ag/AgCl reference electrode and Pt counter electrode at 1.32 V vs. NHE and 1.34 V vs. NHE respectively.

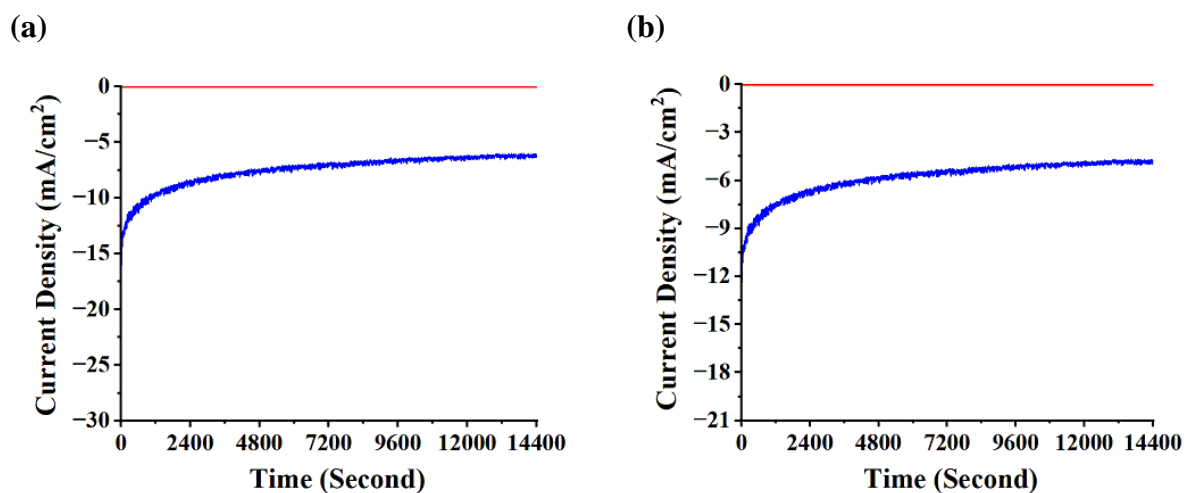


**Fig. S55** Plot of current density vs. time recorded during 4 hour of bulk electrolysis with (blue line) and without (red line) (a) complex **4** and (b) complex **5** in 0.1 M neutral phosphate buffer using ITO working electrode (area 4 cm<sup>2</sup>), Ag/AgCl reference electrode and Pt counter electrode at 1.73 V vs. NHE and 1.75 V vs. NHE respectively.

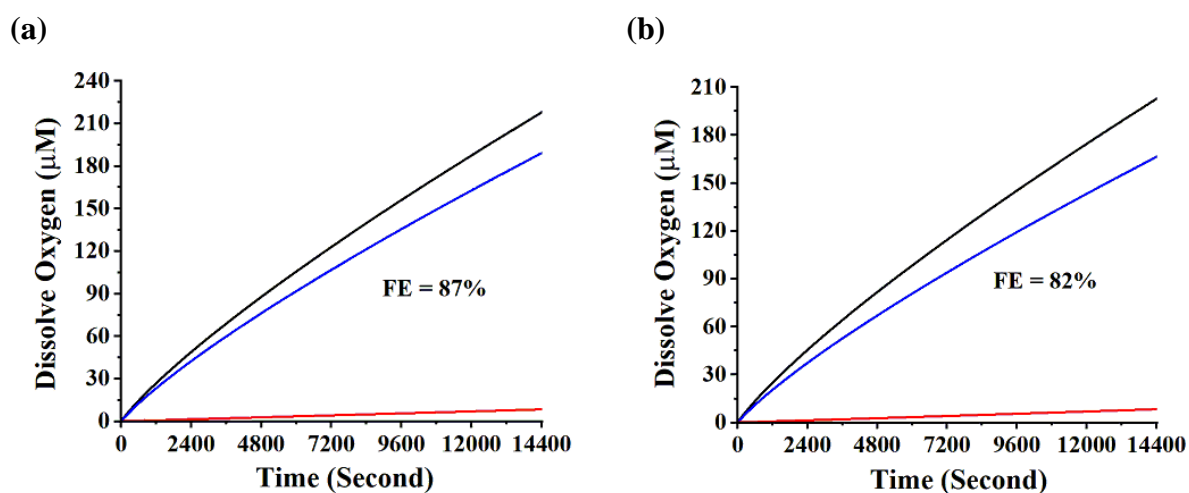


**Fig. S56** Oxygen evolution during the bulk electrolysis with an ITO electrode (area = 4 cm<sup>2</sup>) for (a) complex **4** and (b) complex **5** at 1.73 and 1.75 V vs. NHE respectively for 4 hour with (blue line) and without copper complexes (red line). The black line indicates the theoretical amount of oxygen as assumed by charge passed with 100 % faradic efficiency.

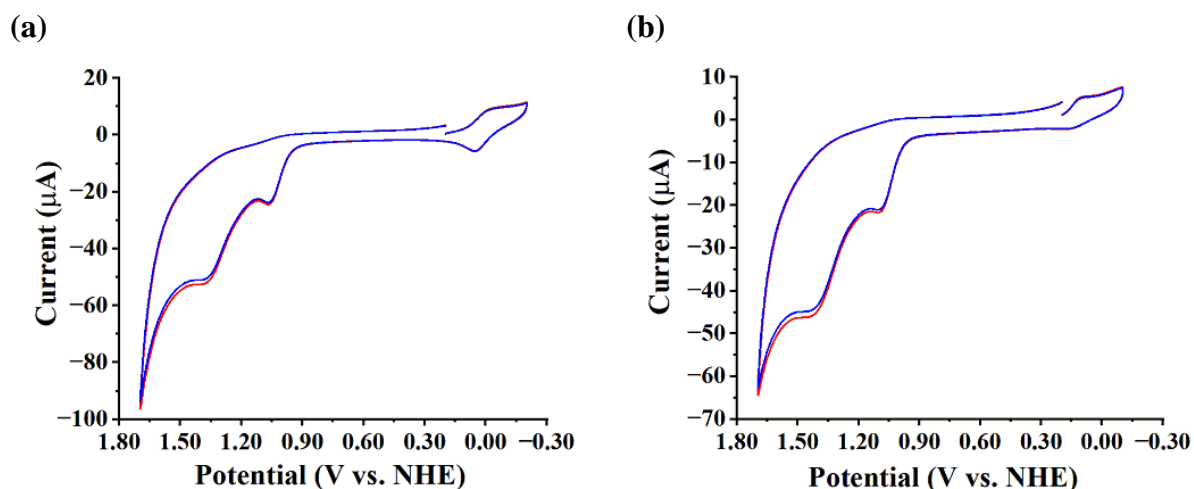


**Fig. S57** Cyclic voltammograms of (a) complex 1 and (b) complex 2 recorded before (red) and after (blue) 4 hour of bulk electrolysis at 1.32 V and 1.34 V vs. NHE respectively in 0.1 M neutral phosphate buffer using glassy carbon (GC) as working electrode (area 0.07 cm<sup>2</sup>), Ag/AgCl as reference electrode and Pt as counter electrode. Scan rate, 100 mVs<sup>-1</sup>.

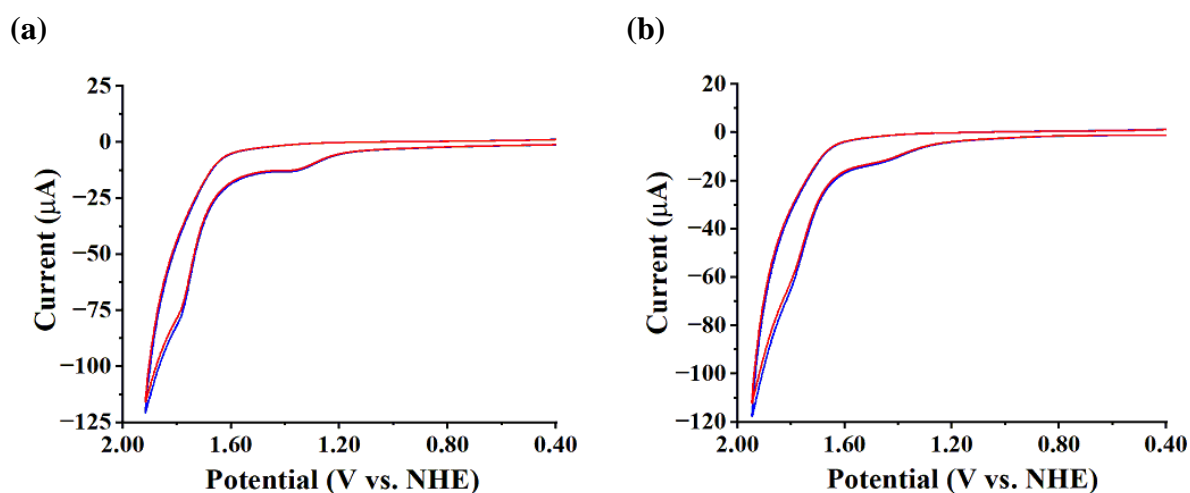


**Fig. S58** Cyclic voltammograms of (a) complex 4 and (b) complex 5 recorded before (blue) and after (red) 4 hour of bulk electrolysis at 1.73 V and 1.75 V vs. NHE respectively in 0.1 M neutral phosphate buffer using glassy carbon (GC) as working electrode (area 0.07 cm<sup>2</sup>), Ag/AgCl as reference electrode and Pt as counter electrode. Scan rate, 100 mVs<sup>-1</sup>.

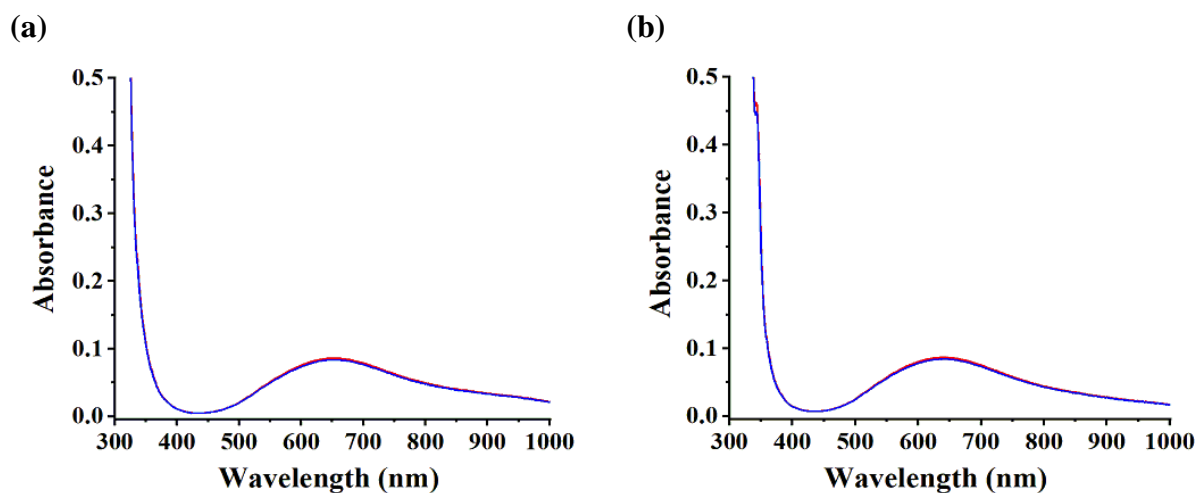


**Fig. S59** UV-visible spectra of (a) complex 1 and (b) complex 2 recorded before (red) and after (blue) 4 hour of bulk electrolysis at 1.32 V and 1.34 V vs. NHE respectively in 0.1 M neutral phosphate buffer.

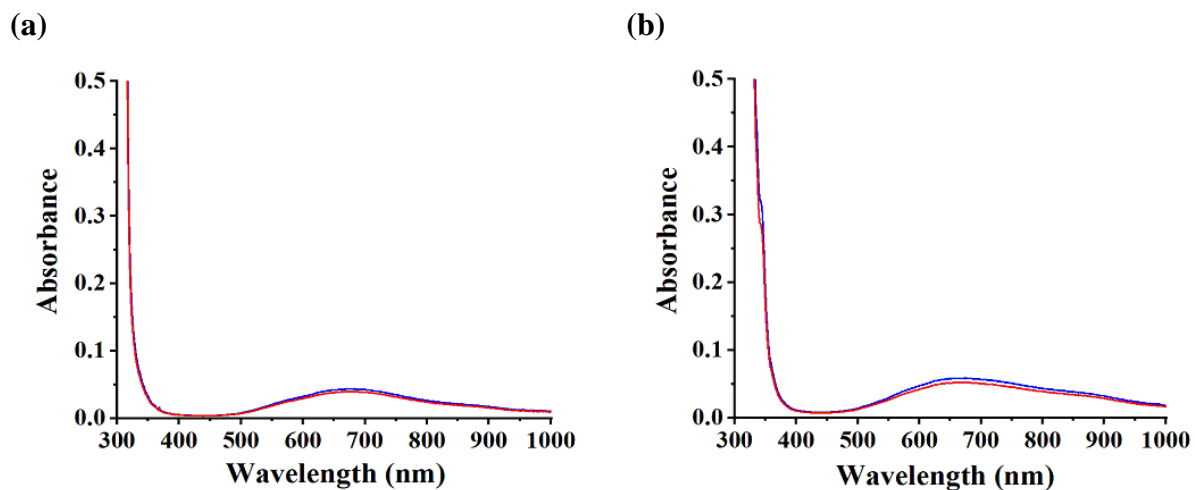


**Fig. S60** UV-visible spectra of (a) complex 4 and (b) complex 5 recorded before (blue) and after (red) 4 hour of bulk electrolysis at 1.73 V and 1.75 V vs. NHE respectively in 0.1 M neutral phosphate buffer.

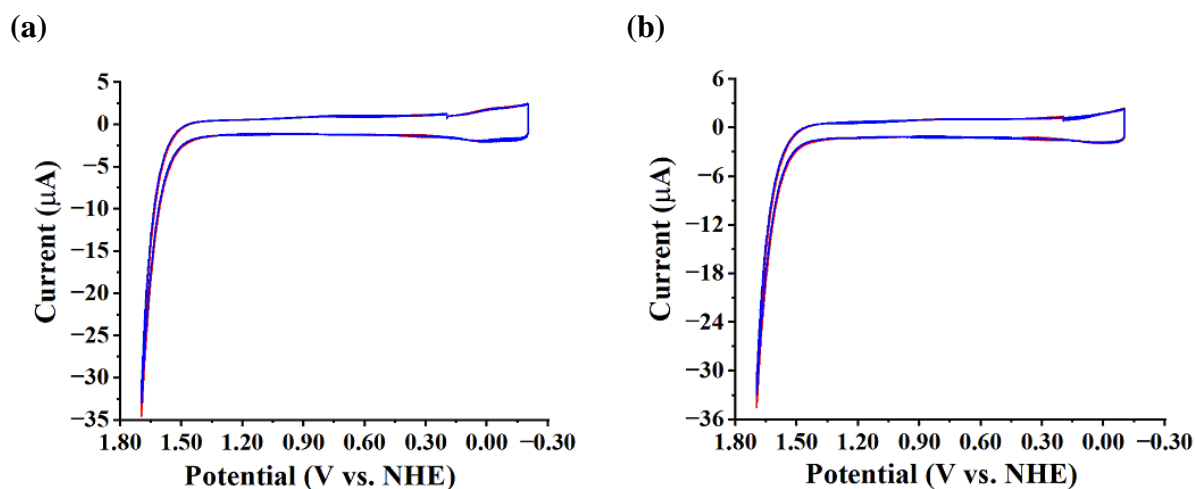


**Fig. S61** Cyclic voltammograms recorded in 0.1 M neutral phosphate buffer in the absence of (a) complex **1** and (b) complex **2** with fresh (red) and used (blue) ITO working electrode (area  $4 \text{ cm}^2$ ), a Ag/AgCl reference electrode and a Pt counter electrode, scan rate,  $100 \text{ mVs}^{-1}$ .

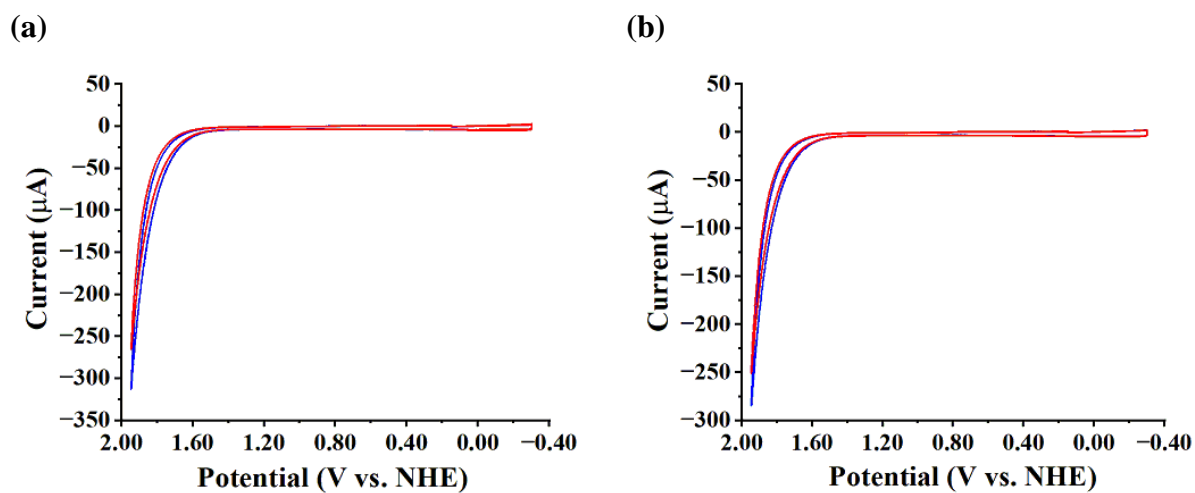


**Fig. S62** Cyclic voltammograms recorded in 0.1 M neutral phosphate buffer in the absence of (a) complex **4** and (b) complex **5** with fresh (blue) and used (red) ITO working electrode (area  $4 \text{ cm}^2$ ), a Ag/AgCl reference electrode and a Pt counter electrode, scan rate,  $100 \text{ mVs}^{-1}$ .

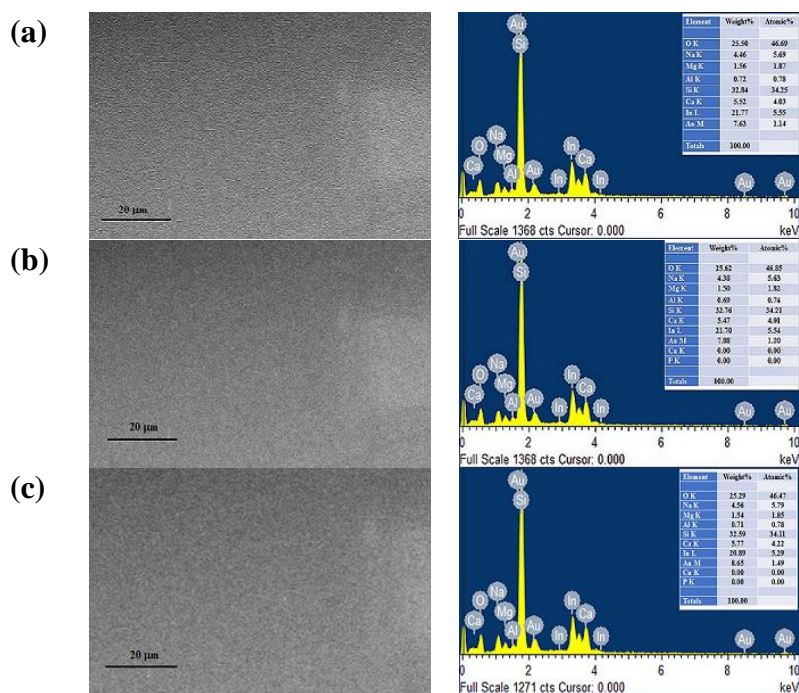


**Fig. S63** FE-SEM and EDX plot of (a) fresh ITO working electrode (b) ITO working electrode after 4 hour of bulk electrolysis of complex 1 and (c) ITO working electrode after 4 hour of bulk electrolysis of complex 2 in 0.1 M neutral phosphate buffer.

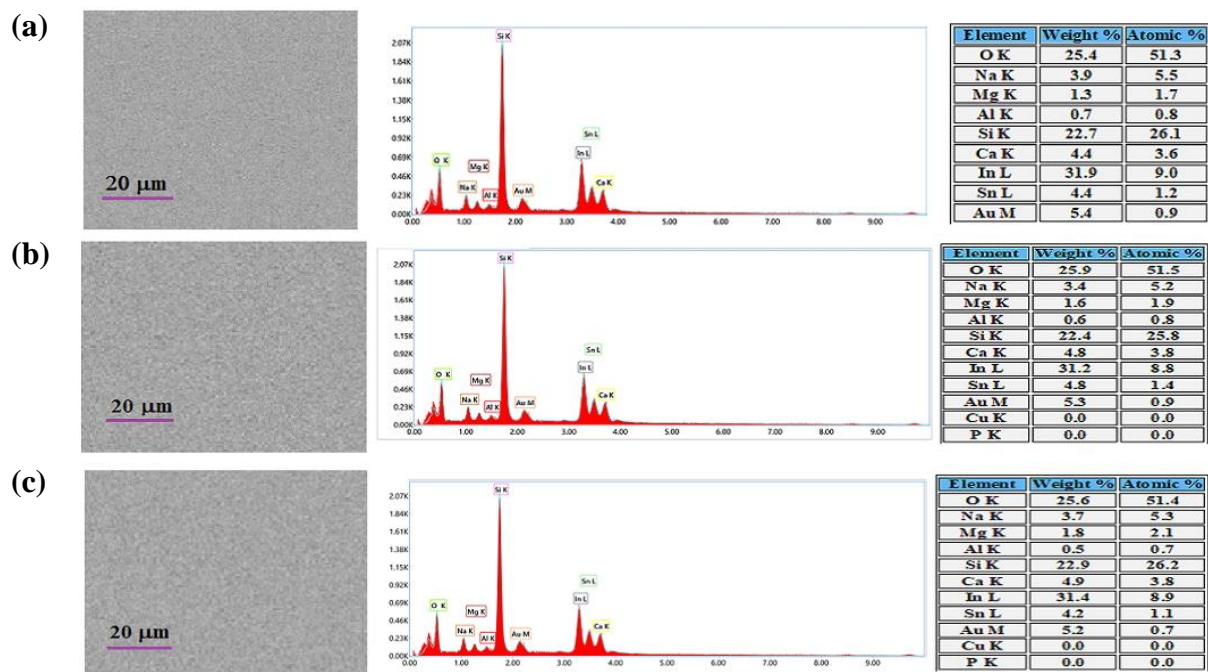


**Fig. S64** FE-SEM and EDX plot of (a) fresh ITO working electrode (b) ITO working electrode after 4 hour of bulk electrolysis of complex **4** and (c) ITO working electrode after 4 hour of bulk electrolysis of complex **5** in 0.1 M neutral phosphate buffer.

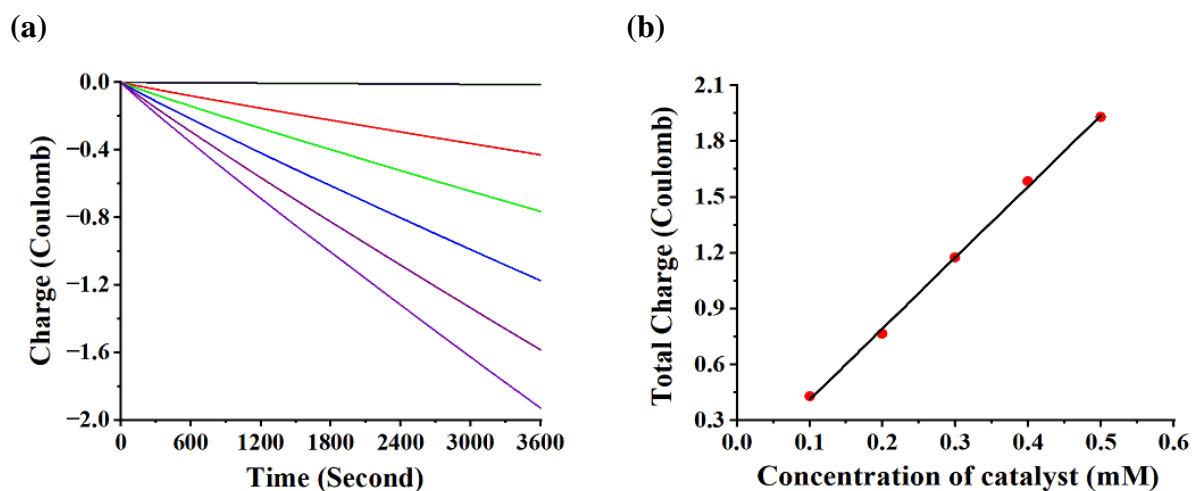


**Fig. S65** (a) Plot of charge vs. time recorded during bulk electrolysis of complex **4** at 0.0 mM (black), 0.1 mM (red), 0.2 mM (green), 0.3 mM (blue), 0.4 mM (purple) and 0.5 mM (violet) concentration at 1.73 V vs. NHE. (b) Plot of total charge vs. concentration of complex **4** after 1 hour of electrolysis.

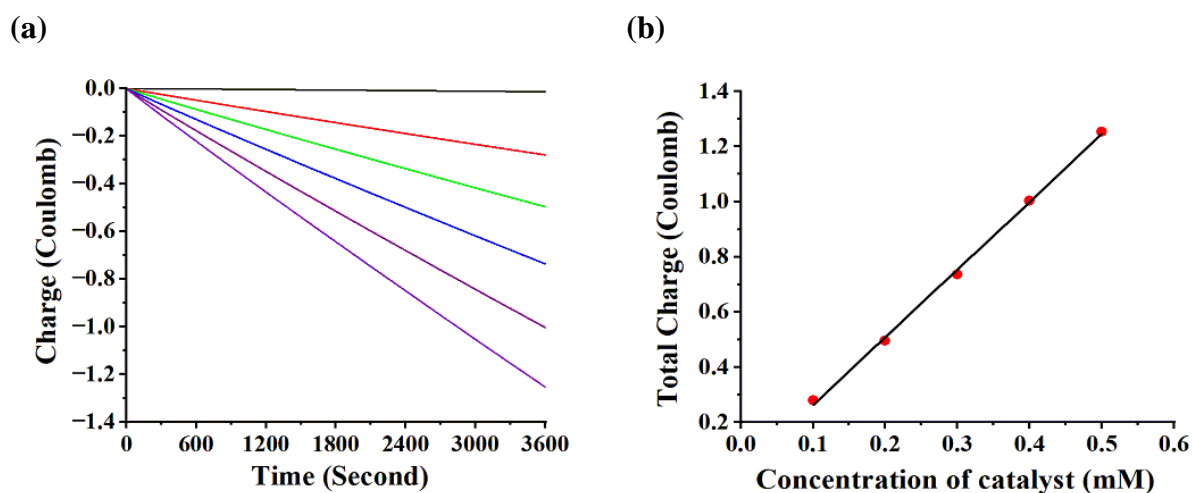


**Fig. S66** (a) Plot of charge vs. time recorded during bulk electrolysis of complex **5** at 0.0 mM (black), 0.1 mM (red), 0.2 mM (green), 0.3 mM (blue), 0.4 mM (purple) and 0.5 mM (violet) concentration at 1.75 V vs. NHE. (b) Plot of total charge vs. concentration of complex **5** after 1 hour of electrolysis.

**Table S1** Crystal data and structure refinement parameters for Complexes **1** and **2**

	<b>Complex 1</b>	<b>Complex 2</b>
Empirical formula	CuC <sub>14</sub> H <sub>21</sub> N <sub>5</sub> Cl <sub>2</sub> O <sub>8</sub>	CuC <sub>16</sub> H <sub>21</sub> N <sub>5</sub> Cl <sub>2</sub> O <sub>8</sub>
Formula weight	521.80	545.83
Wavelength( $\lambda$ )	0.71073 Å	0.71073 Å
Temperature (K)	273(2)	273(2)
Crystal system	Monoclinic	Triclinic
Space group	P 2 <sub>1</sub> /c	P-1
a[Å]	11.2765 (14)	8.135 (2)
b[Å]	12.4838 (17)	10.258 (3)
c[Å]	14.6886 (18)	13.835 (4)
$\alpha$ [°]	90	98.260 (7)
$\beta$ [°]	90.381 (3)	106.413 (7)
$\gamma$ [°]	90	91.759 (8)
Volume[Å <sup>3</sup> ]	2067.7 (5)	1092.9 (6)
Z	4	2
Density [g/cm <sup>3</sup> ]	1.676	1.659
Abs. coeff. [mm <sup>-1</sup> ]	1.367	1.298
F(000)	1068.0	558.0
Reflections collected	34660	26330
R <sub>int</sub>	0.1082	0.0709
Data / restraints / parameters	3639/0/271	3900/100/347
Min. 2 $\theta$ /°	4.282	5.236
Max. 2 $\theta$ /°	49.994	50.276
Ranges (h, k, l)	-13 ≤ h ≤ 13, -14 ≤ k ≤ 14, -17 ≤ l ≤ 17	-9 ≤ h ≤ 9, -12 ≤ k ≤ 12, -16 ≤ l ≤ 16
Complete to 2 $\theta$ (%)	100.0	99.6
Goof (F <sup>2</sup> )	1.036	1.052
Final R indices [I>=2 $\sigma$ (I)]	R <sub>1</sub> = 0.0435, wR <sub>2</sub> = 0.1064	R <sub>1</sub> = 0.0409, wR <sub>2</sub> = 0.0877
R indices (all data)	R <sub>1</sub> = 0.0536, wR <sub>2</sub> = 0.1147	R <sub>1</sub> = 0.0592, wR <sub>2</sub> = 0.0972
CCDC No.	2401171	2401172

**Table S2** Crystal data and structure refinement parameters for Complexes **3** and **4**

	<b>Complex 3</b>	<b>Complex 4</b>
Empirical formula	CuC <sub>4</sub> H <sub>12</sub> N <sub>3</sub> Br <sub>2</sub>	CuC <sub>22</sub> H <sub>21</sub> N <sub>5</sub> Cl <sub>2</sub> O <sub>8</sub>
Formula weight	325.52	617.88
Wavelength( $\lambda$ )	0.71073	0.71073
Temperature (K)	273(2)	293(2)
Crystal system	Orthorhombic	Monoclinic
Space group	Pmmn	P 2 <sub>1</sub> /c
a[Å]	8.702(4)	11.7537(16)
b[Å]	6.252(3)	9.5153(13)
c[Å]	8.543(3)	23.375(3)
$\alpha$ [°]	90	90
$\beta$ [°]	90	100.793(6)
$\gamma$ [°]	90	90
Volume[Å <sup>3</sup> ]	464.8(3)	2568.0(6)
Z	2	4
Density [g/cm <sup>3</sup> ]	2.326	1.598
Abs. coeff. [mm <sup>-1</sup> ]	10.883	1.115
F(000)	312.0	1260.0
Reflections collected	8389	64490
R <sub>int</sub>	0.0589	0.0497
Data / restraints / parameters	497/1/41	4507 / 0 / 343
Min. 2 $\theta$ /°	4.768	4.510
Max. 2 $\theta$ /°	50.434	49.996
Ranges (h, k, l)	-10 ≤ h ≤ 10 -7 ≤ k ≤ 7 -10 ≤ l ≤ 10	-13 ≤ h ≤ 13 -11 ≤ k ≤ 11 -27 ≤ l ≤ 27
Complete to 2 $\theta$ (%)	99.8	100.0
Goof (F <sup>2</sup> )	1.153	1.081
Final R indices [I >= 2 $\sigma$ (I)]	R <sub>1</sub> = 0.0257, wR <sub>2</sub> = 0.0565	R <sub>1</sub> = 0.0380, wR <sub>2</sub> = 0.0983
R indices (all data)	R <sub>1</sub> = 0.0308, wR <sub>2</sub> = 0.0585	R <sub>1</sub> = 0.0480, wR <sub>2</sub> = 0.1066
CCDC No.	2435313	2435314

**Table S3** Crystal data and structure refinement parameters for Complexes **5** and **6**

	<b>Complex 5</b>	<b>Complex 6</b>
Empirical formula	CuC <sub>24</sub> H <sub>21</sub> N <sub>5</sub> Cl <sub>2</sub> O <sub>8</sub>	CuC <sub>25</sub> H <sub>19</sub> N <sub>5</sub> Cl <sub>2</sub> O <sub>8</sub>
Formula weight	641.90	651.89
Wavelength( $\lambda$ )	0.71073	0.71073
Temperature (K)	296(2)	293(2)
Crystal system	Monoclinic	Triclinic
Space group	P2 <sub>1</sub> /n	P -1
a[Å]	13.234(4)	10.864(5)
b[Å]	9.107(2)	15.501(7)
c[Å]	22.063(6)	15.746(7)
$\alpha$ [°]	90	72.293(11)
$\beta$ [°]	106.596(7)	88.106(13)
$\gamma$ [°]	90	86.467(12)
Volume[Å <sup>3</sup> ]	2548.3(12)	2521(2)
Z	4	4
Density [g/cm <sup>3</sup> ]	1.673	1.718
Abs. coeff. [mm <sup>-1</sup> ]	1.128	1.141
F(000)	1308.0	1324.0
Reflections collected	49156	53883
R <sub>int</sub>	0.0993	0.0779
Data / restraints / parameters	4380/0/361	8721/ 0 / 739
Min. 2 $\theta$ /°	3.852	2.716
Max. 2 $\theta$ /°	49.656	49.994
Ranges (h, k, l)	-15 ≤ h ≤ 15 -10 ≤ k ≤ 10 -25 ≤ l ≤ 26	-12 ≤ h ≤ 12 -18 ≤ k ≤ 18 -18 ≤ l ≤ 18
Complete to 2 $\theta$ (%)	99.6	98.3
Goof (F <sup>2</sup> )	1.020	1.040
Final R indices [I>2 $\sigma$ (I)]	R <sub>1</sub> = 0.0411, wR <sub>2</sub> = 0.0857	R <sub>1</sub> = 0.0386, wR <sub>2</sub> = 0.0864
R indices (all data)	R <sub>1</sub> = 0.0652, wR <sub>2</sub> = 0.0963	R <sub>1</sub> = 0.0636, wR <sub>2</sub> = 0.0980
CCDC No.	2435315	2435316

**Table S4** Crystal data and structure refinement parameters for Complexes  
**[Zn(bipy)(HL<sub>1</sub>)](ClO<sub>4</sub>)<sub>2</sub> and [Zn(phen)(HL<sub>1</sub>)](ClO<sub>4</sub>)<sub>2</sub>**

	<b>[Zn(bipy)(HL<sub>1</sub>)](ClO<sub>4</sub>)<sub>2</sub></b>	<b>[Zn(phen)(HL<sub>1</sub>)](ClO<sub>4</sub>)<sub>2</sub></b>
Empirical formula	ZnC <sub>14</sub> H <sub>21</sub> N <sub>5</sub> Cl <sub>2</sub> O <sub>8</sub>	ZnC <sub>16</sub> H <sub>21</sub> N <sub>5</sub> Cl <sub>2</sub> O <sub>8</sub>
Formula weight	523.63	547.67
Wavelength( $\lambda$ )	0.71073 Å	0.71073 Å
Temperature (K)	296(2)	296(2)
Crystal system	Triclinic	Triclinic
Space group	P-1	P-1
a[Å]	7.908(17)	8.321(6)
b[Å]	10.73(2)	10.361(7)
c[Å]	13.24(3)	13.426(9)
$\alpha$ [°]	102.09(4)	96.255(15)
$\beta$ [°]	105.558(18)	102.884(15)
$\gamma$ [°]	95.97(3)	93.675(14)
Volume[Å <sup>3</sup> ]	1043(4)	1117.0(13)
Z	2	2
Density [g/cm <sup>3</sup> ]	1.668	1.628
Abs. coeff. [mm <sup>-1</sup> ]	1.486	1.391
F(000)	536.0	560.0
Reflections collected	36763	32719
R <sub>int</sub>	0.0590	0.0432
Data / restraints / parameters	3671/0/272	3933/102/354
Min. 2 $\theta$ /°	3.940	3.972
Max. 2 $\theta$ /°	49.994	49.998
Ranges (h, k, l)	-9 ≤ h ≤ 9, -12 ≤ k ≤ 12, -15 ≤ l ≤ 15	-9 ≤ h ≤ 9, -12 ≤ k ≤ 12, -15 ≤ l ≤ 15
Complete to 2 $\theta$ (%)	100.0	99.9
Goof (F <sup>2</sup> )	1.046	1.091
Final R indices [I>2 $\sigma$ (I)]	R <sub>1</sub> = 0.0371, wR <sub>2</sub> = 0.0968	R <sub>1</sub> = 0.0389, wR <sub>2</sub> = 0.0986
R indices (all data)	R <sub>1</sub> = 0.0474, wR <sub>2</sub> = 0.1051	R <sub>1</sub> = 0.0514, wR <sub>2</sub> = 0.1083
CCDC No.	2435317	2435318

## References:

- S1 G. M. Sheldrick, A short history of *SHELX*, *Acta Cryst. A*, 2008, **64**, 112–122.
- S2 G. M. Sheldrick, Crystal structure refinement with *SHELXL*, *Acta Cryst. C*, 2015, **71**, 3–8.
- S3 L. J. Bourhis, O. V. Dolomanov, R. J. Gildea, J. A. K. Howard and H. Puschmann, The anatomy of a comprehensive constrained, restrained refinement program for the modern computing environment – *Olex2* dissected, *Acta Cryst. A*, 2015, **71**, 59–75.
- S4 O. V. Dolomanov, L. J. Bourhis, R. J. Gildea, J. A. K. Howard and H. Puschmann, *OLEX2*: a complete structure solution, refinement and analysis program, *J. Appl. Cryst.*, 2009, **42**, 339–341.